くっつく．そこで受容体に本当のホルモンが作用するのをブロックする働きがあるようなのです．その一つがTGFβだったり，Wntだったりするので，Klothoが減るとWntが働いてstem cell(幹細胞)が減少したり，TGFβだったら線維化をどんどん促進させたりします．そういった意味では，老化，腎硬化が進みやすくなるのではないかと思いますね．

脇野　老化に伴う蛋白が出てくるのですね．

竹中　そういった意味で，CKDでKlothoが下がってくる方は，GFRが落ちるのも早くなる．

先ほども出ましたが，MBDの治療をするとCKDの進行が遅くなる．不思議なことにKlothoをビタミンDが誘導します．Klothoへの作用がビタミンDで予後がよくなることに関与しているのかなと考えていました．最近はエリスロポエチンでKlothoがupregulateされるなど，いろいろなことがいわれていて，おもしろいと思っています．

脇野　最先端のお話をありがとうございます．確かにおっしゃるとおり，普通の人に老化反応が加速して起こるとよくない，そういうイメージですね．

竹中　そうですね．普通の老化はよいけれども，CKDがあって，もっと老化を促進するようなことがあるのはよくない．

脇野　老化している細胞が出していくサイトカインの中には，TGFβもあって，それが線維化の促進に関与する．要するに，普通の老化は静かにTGFβを出して，ゆっくりその組織を線維化して穴を埋める．ところが，それが若い人にどんどん出てくると結局よくない．後でいろいろなサイトカインが悪さをするということです．

CKDの治療の仕方

脇野　研究の最先端を教えていただいたところで，最後に，治療の仕方についてお聞きします．

現在の治療薬で腎疾患の進行をとめるのはACEI，ARBが筆頭で出ていますね．ほかにはエリスロポエチンだとか吸着薬のクレメジンなどが証明されていますが，実地臨床で適用外の薬でも，よいものはありますか．竹中先生，抗老化ビタミンDについては，いかがでしょう．

竹中　リウマチの抗体医療のような画期的な治療が残念ですが腎臓には今までありません．あくまでもKlothoを中心に，リサーチで考えれば，ビタミンDです．Klothoはいろいろな物質で誘導されます．PPARγもその一つだし，スタチン，ビタミンDも，最近はEPOも，どうもそういった作用があるというデータが出ています．同時に，アンジオテンシンⅡはKlothoを抑えるほうですので，ACEI，ARBもKlothoを温存することになります．全部になってしまいますね(笑)．Klotho蛋白は合成できるので，それを打ってあげるのもよいのかもしれませんが，倫理がなかなか許さないというところです．

脇野　柴垣先生はいかがですか．

柴垣　私は実地臨床家にすぎないので，研究段階の治療に関しては，正直，知識がなくてよくわからないのですが，先ほどいいましたように集学的治療が一番重要だし，もう少ししたほうがよいのではないか．ACEI，ARBだけで終わってしまっていないか，あるいは貧血に興味があったときに貧血だけ治して満足していないか．もっと同時進行的にやらなければいけない．

その一方で，高齢者にそういう集学的な治療を行っていくと，いわゆるポリファーマシーという問題が出てきて，そことの兼ね合いにいつも悩みます．こんなに食べるように投薬してよいのだろうかという反省もあるので，個々にバランスをとりながら，その患者さんに合った治療を考えていかなければいけないと思います．

脇野　ベーシックは大事だけれども，その辺のジレンマがあるのですね．

柴垣　もう1点は，どこまで治療するべきなのかということです．とくに高齢者において，正常な老化と病的なものの区別が重要で，つまり，代謝がそこまで高くなくて，高いGFRが必要ないから低下しているのか，実際にGFRが低下して病的なことが起こっているのかという区別が必要です．そこに，先ほど話題となっていたKlothoなどが一つのヒントになったりするのかもしれません．病的なものと正常なものとの違いをもう少しわかりやすいマーカーでみて，それによって，この人は本当に治療が必要なのか，そのレベルからはじめることも，すごく重要ではないでしょうか．

先ほどいいましたように，高齢者の正常の老化でGFRが下がっている方に，ACEI，ARBを使って高カリウム血症になってしまうとか，治療することで患者さんのQOLを下げたり，状態をわるくすることは絶対避けなければいけませんので，そのような臨床に即した研究をしていかなければと思います．

岡田　一つ一つの進行因子に注目していくと，限りなく薬剤が増えてしまうので，重要性を考えて薬物の選択を行う必要があると思います．実際の診療ではガイドラインにすべて従うことはできず，血圧管理一つ取り上げても，降圧目標，薬剤の選択には患者さんそれぞれの病態をみながら考える必要があると思います．とくに高齢者ですでに心血管合併症があるような場合では，腎機能低下抑制だけでなく，さらに合併症を起こさないような全身管理という観点で診療を行う必要があると思います．最近の薬物治療で私が感銘を受けたのは，古典的ではありますが，代謝性アシドーシスの是正による腎機能低下抑制効果に関する報告です(de Brito-Ashurst I et al：J Am Soc Nephrol 20：2075, 2009)．これについては検証する必要があると思います．

脇野　私は基礎研究的なところに話を戻させていただくのですが，最近は腎不全の患者さんのインスリン抵抗性に興味をもっていまして，集中的にやっています．これは，数年前，ドイツのグループがステージ1，ステージ2の患者さんでもHOMA-IRが上がっているというデータを出していますし，eGFRが50を切ると，グルコースクランプをして，腎不全だけでインスリン抵抗性が認められることが示されています．機序としてはビタミンDとか尿毒症とかいわれていますが，私どもはそれをいくつか研究しています．心血管イベントの原因としてのインスリン抵抗性と，腎症進行のファクターとしてのインスリン抵抗性を少し見直したほうがよいのではないかと思います．

そういった意味で，今後期待しているのが，インスリン抵抗性改善薬なのです．最近，アディポネクチンレセプターのノックアウトマウスの腎症のデータが出ていますし，いずれにせよインスリン抵抗性が腎機能をわるくするというデータが出ている．今までRASを中心に話が出ていましたが，肥満などの観点から，インスリンシグナルの管理も今後，腎臓の分野でも，あるいはその腎臓から出てくる心血管イベントの分野でも，重要になってくるのではないかと感じて，そういう薬剤の腎症に対する効果がおもしろいのではないかと考えています．

本日は，基礎から臨床を中心に精力的にされている先生方から広範なご意見をお聞きして，CKDの管理，その問題点，管理の仕方，そしてかなり広まっている方法に対するコントロバーシーや限界，治療に関してお話ししました．血圧，貧血など基本的なリスクファクターの管理は非常に重要だという合意もできて勉強になりました．実地臨床の先生も，専門の先生も非常に啓発されるような内容をいろいろ聞くことができたと思います．どうもありがとうございました．

Science Signaling

Rho and Rho-Kinase Activity in Adipocytes Contributes to a Vicious Cycle in Obesity That May Involve Mechanical Stretch

Yoshikazu Hara, Shu Wakino, Yoshiyuki Tanabe, Maki Saito, Hirobumi Tokuyama, Naoki Washida, Satoru Tatematsu, Kyoko Yoshioka, Koichiro Homma, Kazuhiro Hasegawa, Hitoshi Minakuchi, Keiko Fujimura, Koji Hosoya, Koichi Hayashi, Koichi Nakayama, Hiroshi Itoh

25 January 2011
Volume 4, pp.1-11

AAAS
ADVANCING SCIENCE, SERVING SOCIETY

METABOLISM

Rho and Rho-Kinase Activity in Adipocytes Contributes to a Vicious Cycle in Obesity That May Involve Mechanical Stretch

Yoshikazu Hara,[1] Shu Wakino,[1]* Yoshiyuki Tanabe,[2] Maki Saito,[2] Hirobumi Tokuyama,[1] Naoki Washida,[1] Satoru Tatematsu,[1] Kyoko Yoshioka,[1] Koichiro Homma,[1] Kazuhiro Hasegawa,[1] Hitoshi Minakuchi,[1] Keiko Fujimura,[1] Koji Hosoya,[1] Koichi Hayashi,[1] Koichi Nakayama,[2] Hiroshi Itoh[1]

The development of obesity involves multiple mechanisms. Here, we identify adipocyte signaling through the guanosine triphosphatase Rho and its effector Rho-kinase as one such mechanism. Mice fed a high-fat diet (HFD) showed increased Rho-kinase activity in adipose tissue compared to mice fed a low-fat diet. Treatment with the Rho-kinase inhibitor fasudil attenuated weight gain and insulin resistance in mice on a HFD. Transgenic mice overexpressing an adipocyte-specific, dominant-negative form of RhoA (DN-RhoA TG mice) showed decreased Rho-kinase activity in adipocytes, decreased HFD-induced weight gain, and improved glucose metabolism compared to wild-type littermates. Furthermore, compared to HFD-fed wild-type littermates, DN-RhoA TG mice on a HFD showed decreased adipocyte hypertrophy, reduced macrophage recruitment to adipose tissue, and lower expression of mRNAs encoding various adipocytokines. Lipid accumulation in cultured adipocytes was associated with increased Rho-kinase activity and increased abundance of adipocytokine transcripts, which was reversed by a Rho-kinase inhibitor. Direct application of mechanical stretch to mature adipocytes increased Rho-kinase activity and stress fiber formation. Stress fiber formation, which was also observed in adipocytes from HFD-fed mice, was prevented by Rho-kinase inhibition and in DN-RhoA TG mice. Our findings indicate that lipid accumulation in adipocytes activates Rho to Rho-kinase (Rho–Rho-kinase) signaling at least in part through mechanical stretch and implicate Rho–Rho-kinase signaling in inflammatory changes in adipose tissue in obesity. Thus, inhibition of Rho–Rho-kinase signaling may provide a therapeutic strategy for disrupting a vicious cycle of adipocyte stretch, Rho–Rho-kinase signaling, and inflammation of adipose tissue that contributes to and aggravates obesity.

INTRODUCTION

A growing body of evidence has implicated obesity as a major risk factor for cardiovascular disease. Many factors, including chronic inflammation, contribute to metabolic syndrome (*1*), a condition characterized by metabolic and circulatory complications of obesity that predispose to the development of type 2 diabetes and cardiovascular disease. Obesity is associated with increased lipid accumulation in adipocytes; adipocytes store this increased lipid as fat deposits, leading to adipocyte hypertrophy. These hypertrophic adipocytes secrete cytokines that have been implicated in various obesity-related disorders, including cardiovascular disease (*2*). These cytokines, called adipocytokines, include bioactive molecules specific to adipocytes, such as adiponectin, as well as proinflammatory cytokines, such as tumor necrosis factor–α (TNFα) and monocyte chemoattractant protein–1 (MCP-1) (*3*). In obesity, adipose tissue is also infiltrated by inflammatory cells, especially monocytes and macrophages (*4*), which may be recruited by chemotactic signals produced by expanding adipocytes or their neighboring preadipocytes (*5*). These infiltrating inflammatory cells secrete cytokines, which in turn affect adipocyte phenotype and accelerate adipocytokine production (*4*). However, the molecular mechanisms that link all of these obesity-related changes—that is to say, adipocyte hypertrophy, abnormal adipocytokine secretion, and the associated inflammatory changes in adipose tissue—remain to be fully elucidated.

The small monomeric guanosine triphosphatase (GTPase) Rho is a critical modulator of vascular smooth muscle cell (VSMC) contraction. Signaling through Rho and its downstream effector Rho-associated kinase (Rho-kinase, also known as ROCK, and consisting of two functionally distinct isoforms) increases myosin light-chain phosphorylation and thereby contributes to agonist-induced Ca^{2+} sensitization in VSMC contraction (*6*) and, consequently, to the pathogenesis of hypertension (*7*). Mechanical stress, including cyclic stretch (*8*) and shear stress (*9*), activates the Rho to Rho-kinase (Rho–Rho-kinase) pathway in the cardiovascular system, as do various vasoactive substances. In cardiomyocytes, RhoA, a member of the Rho family, is pivotal to the progression of stretch-induced cellular hypertrophy (*10*). The Rho–Rho-kinase pathway, which promotes insulin resistance and thus decreases glucose tolerance (*11*), is activated in muscle tissue in obese Zucker rats (*11*). Rho–Rho-kinase signaling leads to serine phosphorylation of insulin receptor substrate 1 (IRS-1) and, consequently, to reduced insulin-stimulated IRS-1 tyrosine phosphorylation and protein kinase B (Akt) activation and thereby to muscle insulin resistance. The Rho-kinase inhibitor fasudil attenuates serine phosphorylation of IRS-1 in obese Zucker rats, with a concomitant improvement in glucose metabolism (*11*). Fasudil also attenuates adipocyte hypertrophy and decreases TNFα and MCP-1 abundance and macrophage infiltration in white adipose tissue (WAT) (*11*). However, whether these represent direct effects of fasudil in adipose tissue or are secondary to increased systemic insulin sensitivity remains unclear.

[1]Department of Internal Medicine, School of Medicine, Keio University, Shinjuku-ku, Tokyo 160-8582, Japan. [2]Department of Molecular and Cellular Pharmacology, School of Pharmaceutical Sciences, Iwate Medical University, Iwate 028-3694, Japan. *To whom correspondence should be addressed. E-mail: swakino@sc.itc.keio.ac.jp

Here, we investigated whether activation of Rho-kinase in adipose tissue participates in the development of obesity. Because Rho can be activated by mechanical stress, we hypothesized that the Rho–Rho-kinase pathway might be activated as mature adipocytes become hypertrophic in obesity. We showed that mechanical stretch to adipocytes was, indeed, a trigger for activation of the Rho–Rho-kinase pathway in adipose tissue, and identified this pathway as a culprit in the initiation and progression of obesity and its pathological complications.

RESULTS

Effects of the Rho-kinase inhibitor fasudil on the phenotype of diet-induced obesity

We first examined the effects of the Rho-kinase inhibitor fasudil in mouse models of diet-induced obesity. C57BL/6J mice maintained on a high-fat diet (HFD) for 12 weeks weighed more than mice fed a low-fat diet (LFD). Although fasudil at 3 mg per kilogram of body weight per day had no effect on body weight, 30 mg/kg per day attenuated the increase in body weight of C57BL/6J mice fed a HFD (Table 1). There was no difference in food intake among these four groups (mice fed a LFD and mice fed a HFD with or without fasudil, 3 or 30 mg/kg per day). Epididymal WAT weighed less in mice fed a HFD treated with fasudil (30 mg/kg per day) than in mice fed a HFD without fasudil, whereas a dosage of 3 mg/kg per day had no effect on epididymal WAT weight (Table 1). Although serum concentrations of triglyceride were not altered among the three groups fed a HFD, increases in total serum cholesterol concentration and serum free fatty acid concentration in response to a HFD were attenuated by fasudil at a dosage of 30 mg/kg per day. These data indicate that 30 mg/kg per day attenuated the initiation or progression (or both) of HFD-induced obesity.

Mice fed a HFD showed glucose intolerance, as evaluated by intraperitoneal glucose tolerance test (ipGTT); glucose tolerance was improved by both fasudil dosages of 3 and 30 mg/kg per day (Fig. 1A). Intraperitoneal insulin injection lowered serum glucose concentration in mice fed a LFD, an effect that was blunted in mice on a HFD (Fig. 1B). Both dosages of 3 and 30 mg/kg per day restored the response to insulin challenge to a degree comparable to that of mice on a LFD (Fig. 1B). These results demonstrated favorable effects by fasudil on systemic glucose metabolism, which could not be ascribed simply to secondary effects of reduced fat mass or body weight.

Effects of the Rho-kinase inhibitor fasudil on adipose tissue in diet-induced obesity

Adipocyte size was increased in mice fed a HFD compared with that in mice fed a LFD. This change was attenuated by a fasudil dosage of 30 mg/kg per day (Fig. 1C). Macrophage infiltration of adipose tissue was also increased in mice fed a HFD, and this was reduced by both dosages of fasudil (Fig. 1D). Abundance of the mRNA transcripts encoding the adipocytokines MCP-1 and TNFα was increased in adipose tissue of mice fed a HFD compared to mice fed a LFD, increases that were attenuated at both concentrations of fasudil. Conversely, abundance of the mRNA encoding adiponectin was decreased in mice on a HFD, a change that was partially reversed at both concentrations of fasudil (Fig. 1E). These data indicate that hypertrophic changes of adipocytes, macrophage migration into adipose tissue, and dysregulation of adipocytokine expression that occur in HFD-induced obesity depend on signaling through the Rho–Rho-kinase pathway.

Attenuation of the aberrant adipocyte phenotype in diet-induced obesity by adipocyte-specific inhibition of Rho–Rho-kinase signaling

The inhibitory effects of fasudil on several aspects of the aberrant phenotype associated with diet-induced obesity suggested that the Rho–Rho-kinase pathway was activated in adipose tissues of obese mice. Immunoblot analysis with an antibody directed against the phosphorylated form of myosin phosphatase target subunit (MYPT), a substrate of Rho-kinase, indicated that Rho-kinase was active in adipose tissue of mice fed a HFD, and that this was inhibited by systemic fasudil (Fig. 1F). Subfractionation of adipose tissues into a stromal vascular fraction (SVF) and a mature adipocyte fraction revealed that activation of Rho-kinase in the adipose tissue of HFD-fed mice occurred mostly in mature adipocytes rather than in macrophages or vascular cells (Fig. 1G).

To delineate the pathological relevance of the activation of Rho–Rho-kinase pathway in adipocytes, we explored the effects of a HFD in transgenic mice in which Rho activation was specifically blocked in adipose tissue. We generated transgenic mice that expressed a dominant-negative human RhoA (DN-RhoA) mutant driven by the promoter of the adipose tissue–specific protein, adipocyte fatty acid binding protein (aP2) (DN-RhoA TG mice) (Fig. 2, A and B). DN-RhoA TG mice were of normal birth weight and were fertile, and the mutant gene was specifically expressed in adipose tissue (Fig. 2C). The following analyses were performed on DN-RhoA TG mice and wild-type littermates fed a HFD. At 18 weeks of age, Rho-kinase activity was specifically decreased in the adipose tissue of DN-RhoA TG mice compared with that of wild-type littermates, as assessed by phosphorylation of the Rho-kinase substrates MYPT and ERM (ezrin, radixin, and moesin) (Fig. 2, D and E, respectively), but was not altered in other tissues. The increase in body weight of DN-RhoA TG mice was significantly attenuated compared with that of wild-type littermates (Fig. 3A). In ipGTT, glucose tolerance was enhanced in DN-RhoA TG mice compared to wild-type mice (Fig. 3B), and serum concentrations of free fatty acid were lower (Fig. 3C). In addition, increases in adipocyte size (Fig. 3D) and infiltration of macrophages in adipose tissue (Fig. 3E) observed in HFD-fed wild-type mice, as well as the

Table 1. Basal characteristics of mice fed a low-fat diet (LFD), high-fat diet (HFD), or HFD plus fasudil (HFD + F3, HFD + F30). F3, 3 mg of fasudil per kilogram of body weight per day; F30, 30 mg of fasudil per kilogram of body weight per day; TC, total cholesterol; TG, triglyceride; FFA, free fatty acid. $^{**}P < 0.01$ versus LFD; $^{\#\#}P < 0.01$ versus HFD; $n = 6$.

	LFD	HFD	HFD + F3	HFD + F30
Body weight (g)	28.7 ± 0.75	43.95 ± 2.55**	42.88 ± 2.93	38.15 ± 1.95##
WAT weight (g)	0.67 ± 0.13	2.24 ± 0.17**	2.18 ± 0.19	1.52 ± 0.12##
TC (mg/dl)	72 ± 12	147 ± 22**	147 ± 18.5	95 ± 15##
TG (mg/dl)	35.6 ± 6.9	48.0 ± 12.0	50.5 ± 8.3	49.0 ± 2.1
FFA (meq/liter)	0.51 ± 0.12	1.02 ± 0.15**	0.712 ± 0.17##	0.66 ± 0.11##

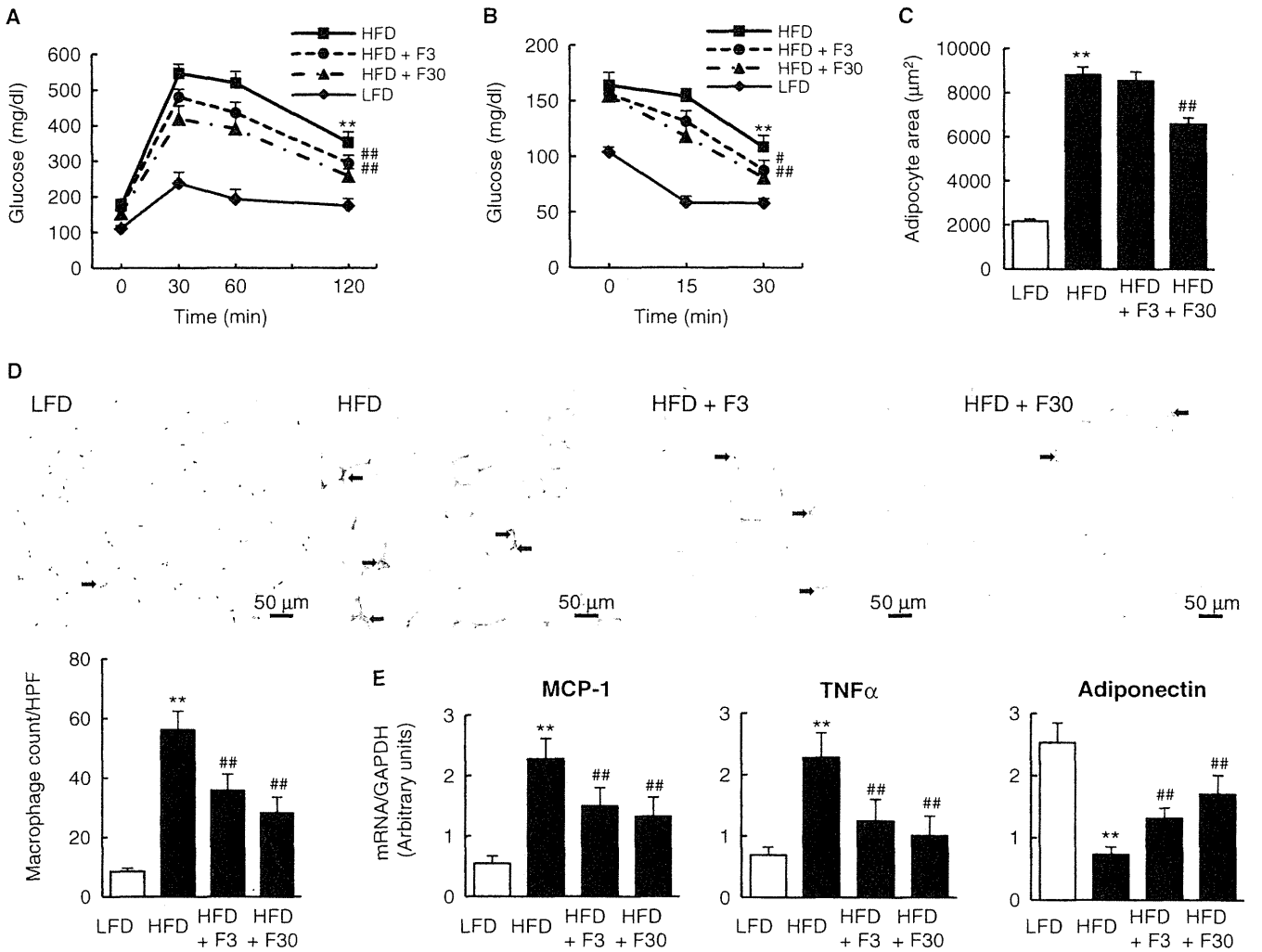

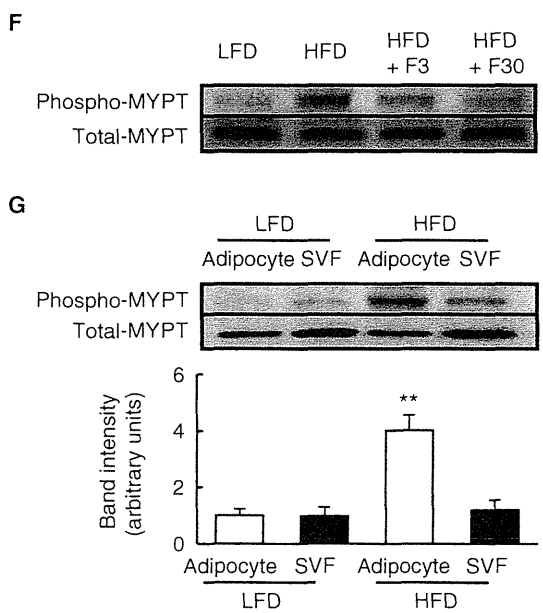

Fig. 1. The effects of the Rho-kinase inhibitor fasudil on glucose tolerance, insulin sensitivity, and adipose tissue of C57BL/6J mice fed a HFD. (A and B) C57BL/6J mice fed a HFD, LFD, and HFD with fasudil, 3 mg/kg (HFD + F3) or 30 mg/kg (HFD + F30), for 3 months; glucose metabolism was evaluated by ipGTT (A) and intraperitoneal insulin tolerance test (B). The concentrations of glucose were compared statistically. $^{**}P < 0.01$ versus LFD, $^{\#\#}P < 0.01$ versus HFD, $^{\#}P < 0.05$ versus HFD. $n = 5$. (C) Adipocyte size in WAT of each group is shown. $^{**}P < 0.01$ versus LFD, $^{\#\#}P < 0.01$ versus HFD. $n = 5$. (D) Number of infiltrated macrophages in adipose tissue, counted under a microscope with a 400× objective. The upper panels show immunostaining with F4/80 antibody against macrophage-specific antigen. Arrows point to individual macrophages. $^{**}P < 0.01$ versus LFD, $^{\#\#}P < 0.01$ versus HFD. $n = 5$. HPF, high-power field. (E) Effects of fasudil on expression of mRNA encoding adipocytokine, MCP-1, TNFα, and adiponectin. $^{**}P < 0.01$ versus LFD, $^{\#\#}P < 0.01$ versus HFD. $n = 5$. (F) Immunoblotting for phospho-MYPT as a marker for Rho-kinase activity. (G) After the mature adipocytes were separated from the stromal vascular fraction, Rho-kinase activity was assessed by immunoblot. $^{**}P < 0.01$ versus LFD, $n = 4$.

abnormal pattern of adipocytokine mRNA abundance (Fig. 3F), were significantly attenuated in DN-RhoA TG mice. To control for effects of body weight on glucose tolerance and insulin sensitivity, we performed ipGTT on 11-week-old mice, a time point when body weight did not differ between the two groups (wild type, 29.4 ± 3.1 g; DN-RhoA TG, 27.2 ± 2.3 g; n = 5). As shown in Fig. 3, G and H, fasting glucose concentrations were higher in wild-type mice (wild type versus DN-RhoA TG: 154 ± 18 mg/dl versus 131 ± 14 mg/dl, $P < 0.05$, $n = 5$), as were fasting insulin concentrations (wild type versus DN-RhoA TG: 424 ± 36 pg/ml versus 308 ± 24 pg/ml, $P < 0.01$, $n = 5$). In addition, glucose tolerance was improved in 11-week-old DN-RhoA TG mice compared with that of wild-type mice (Fig. 3G), and DN-RhoA TG mice were also more insulin-sensitive (Fig. 3H). Thus, DN-RhoA TG mice were more insulin-sensitive and had improved glucose tolerance independent of body weight.

Treatment with fasudil at 30 mg/kg per day did not further improve glucose tolerance or insulin sensitivity in 11-week-old DN-RhoA TG mice (Fig. 3, G and H). Thus, RhoA activation in adipocytes appears to be critical for Rho-kinase activation–induced systemic insulin resistance in obesity. Together, these data indicate that the activation of Rho–Rho-kinase pathway in the adipose tissue directly promotes the hypertrophic adipocyte phenotype in HFD-induced obesity.

Rho-kinase activation in hypertrophic adipocytes

We investigated the mechanism for the activation of Rho–Rho-kinase signaling in an in vitro model in which 3T3-L1 fibroblasts were exposed to factors that promoted their differentiation into adipocytes (see Materials and Methods). Before adipocytic differentiation (day 8 of exposure to differentiating agents), Rho-kinase activity was low. Rho-kinase activity increased after differentiation and as lipid accumulated and cells increased in size (Fig. 4, A and B). Rho-kinase activation induces the expression of cytokines and chemokines including MCP-1 (*12*) and TNFα (*13*). Consistent with this, the abundance of the mRNAs encoding MCP-1 and TNFα was increased in adipocytes at days 12 and 16. These increases in mRNA abundance were inhibited by the Rho-kinase inhibitor Y-

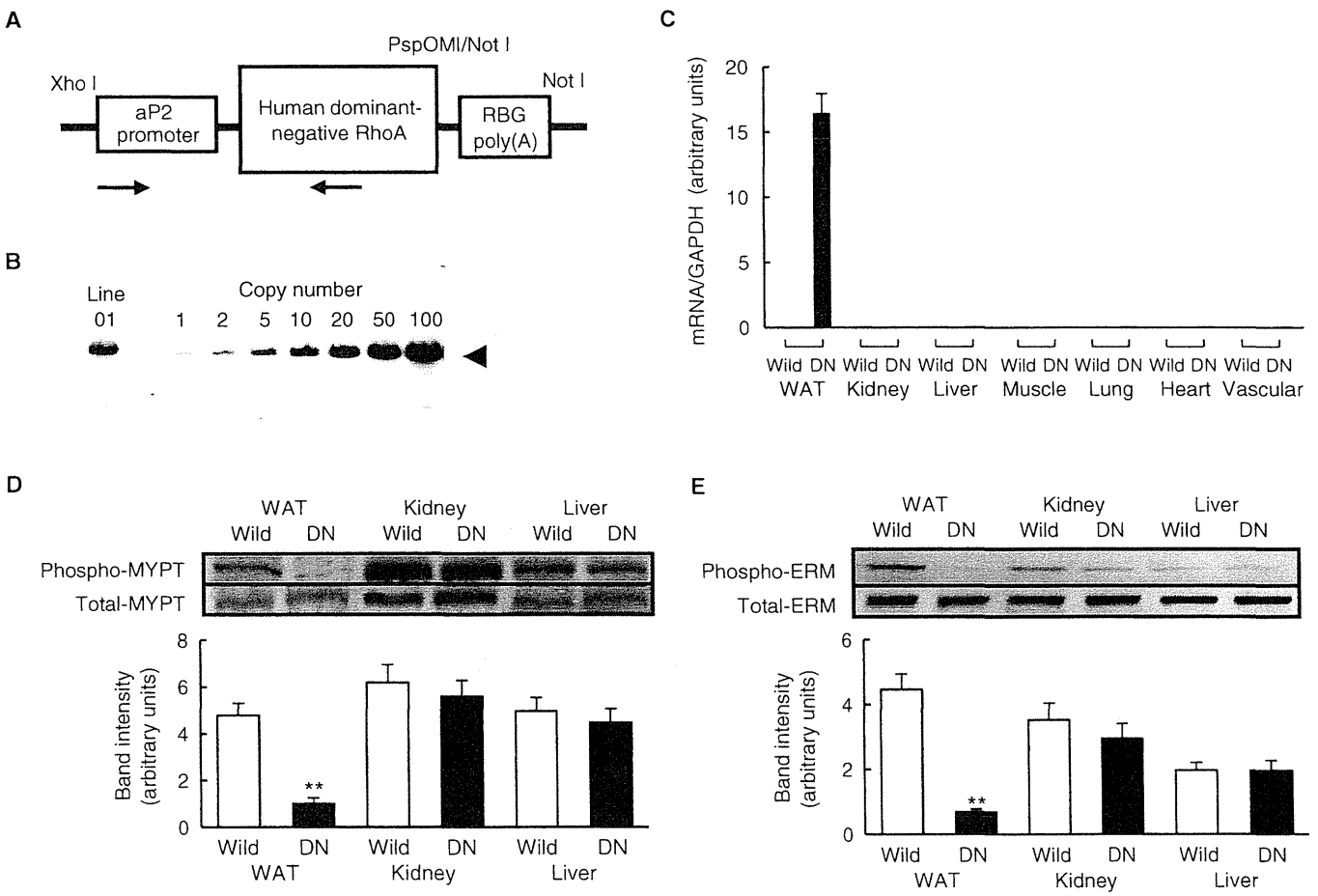

Fig. 2. Generation of transgenic mice with adipose tissue–specific dominant-negative human RhoA. (A) The construct used for the generation of adipose tissue–specific dominant-negative human RhoA transgenic (DN-RhoA TG) mice. A fragment composed of the aP2 promoter, human DN-RhoA cDNA, and RBG poly(A) sequences was excised from aP2 promoter vector by Xho I and Not I and injected into one-cell fertilized mouse embryos obtained from superovulated C57BL/6 × C3H mice for the production of TG mice. The primers used for genotyping in PCR are indicated as arrows. (B) Southern blot analysis shows 13 copies of the RhoA transgene in mice of line 01. An arrow indicates bands corresponding to transgene-derived RhoA. Transgenic vector including human DN-RhoA genes used as a positive control. (C) Real-time PCR analysis with specific primers shows the presence or absence of mRNA for DN-RhoA in various tissues. DN, DN-RhoA TG mice; Wild, wild-type mice. $n = 4$. (D and E) Immunoblot analysis of phospho-MYPT (D) and phospho-ERM (E). $^{**}P < 0.01$ versus wild type, $n = 4$. (D) and (E) indicate that the Rho-kinase activity is specifically inhibited in WAT in DN-RhoA TG mice.

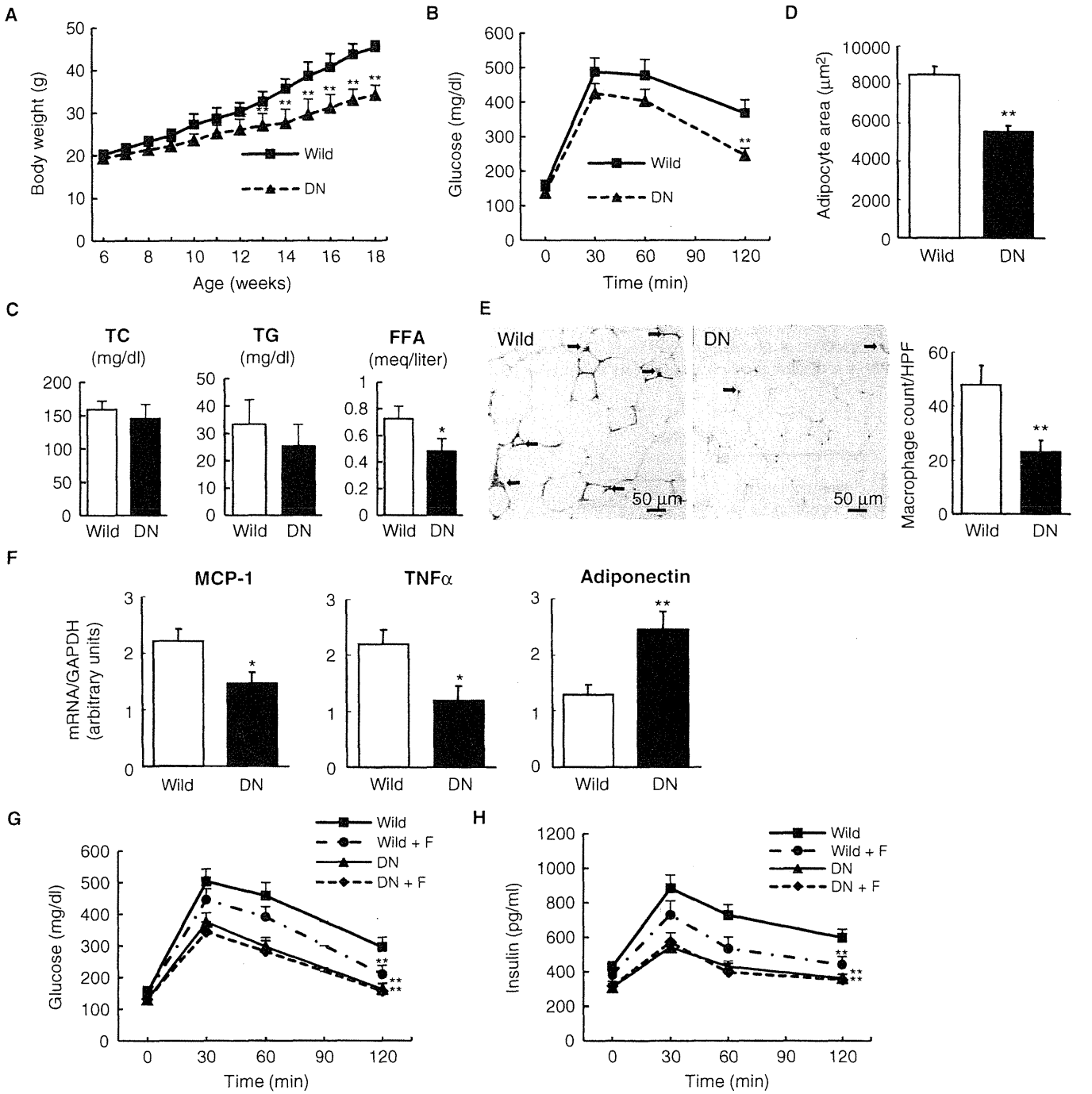

Fig. 3. Phenotype of DN-RhoA TG mice and wild-type littermates. (A) Weight gain of DN-RhoA TG mice (DN) and wild-type littermates (Wild) fed a HFD for 12 weeks, from 6 to 18 weeks of age. $^{**}P < 0.01$ versus wild type, $n = 5$. (B) ipGTT of DN and wild type at 18 weeks of age. $^{**}P < 0.01$ versus wild type, $n = 5$. (C) Serum concentrations of lipid of DN and wild type at 18 weeks of age. $^{*}P < 0.05$ versus wild type, $n = 8$. (D) Adipocyte size in WATs of DN and wild type at 18 weeks of age. $^{**}P < 0.01$ versus wild type, $n = 5$. (E) Number of infiltrating macrophages (arrows) in adipose tissue of DN and wild type at 18 weeks of age, counted under a microscope with a 400× objective. The left panels show immunostaining of F4/80 antibody against macrophage-specific antigen. $^{**}P < 0.01$ versus wild type. HPF, high-power field. (F) mRNA encoding MCP-1, TNFα, and adiponectin in adipose tissues of DN and wild type at 18 weeks of age. $^{*}P < 0.05$ versus wild type, $^{**}P < 0.01$ versus wild type. $n = 5$. (G and H) ipGTT with HFD-fed DN and wild type at 11 weeks of age, a point when the body weight did not differ significantly between the two groups. ipGTT was also performed on mice treated with fasudil (30 mg/kg per day). Glucose concentrations (G) and insulin concentrations (H) were measured during ipGTT. $^{**}P < 0.01$ versus wild, $n = 5$. "F" represents 30 mg of fasudil per kilogram of body weight per day treatment.

27632 (Fig. 4C). The expression of adiponectin was decreased in adipocytes at day 16, a change that was also reversed by Y-27632 (Fig. 4C). Similar results were obtained in experiments with fasudil as a Rho-kinase inhibitor instead of Y-27632 (fig. S1). These data indicate that, as adipocytes increase in size, Rho-kinase activity increases, leading to altered adipocytokine expression.

Stretch-induced Rho-kinase activation and stress fiber formation in mature adipocytes

To explore the mechanisms underlying Rho-kinase activation in hypertrophic adipocytes, we examined the effects of mechanical stretch on Rho-kinase activation in mature adipocytes. Our data with the DN-RhoA TG mice indicated that an ~50% increase in adipocyte area, corresponding to an ~20% increase in diameter, provided sufficient mechanical stress to elicit adipocyte biochemical responses. Therefore, we stretched mature adipocytes grown on a silicon substratum up to 120% of initial diameter for 72 hours and investigated the effects on Rho-kinase activity. We found that Rho-kinase was activated after this constant, long-lasting stretch (Fig. 5A). Furthermore, the expression of the mRNA encoding adiponectin was decreased 43% and that of the mRNA encoding MCP-1 was increased 60% in stretched adipocytes compared with their expression in non-stretched adipocytes ($P < 0.01$, $n = 5$). These results were similar to those obtained in vivo in the diet-induced obese mice and the DN-RhoA TG mice models (Figs. 1E and 3F). Staining of the Rho-kinase effector F-actin was increased in stress fibers by mechanical stretch (Fig. 5B), indicating that Rho-kinase was activated in stretched adipocytes and induced stress fiber reorganization. F-actin staining of adipose tissue was increased in HFD-fed mice, and this was attenuated by the Rho-kinase inhibitor fasudil (Fig. 5C). F-actin staining was also decreased in adipose tissue of DN-RhoA TG mice compared with that of wild-type mice (Fig. 5D). Measurements of cellular size indicated that F-actin–positive adipocytes were larger in size than F-actin–negative cells, providing a link between Rho-kinase activity and adipocyte size (Fig. 5, C and D, lower right panel).

DISCUSSION

The small GTPase Rho and its downstream effector Rho-kinase were initially identified as mediators of vascular contraction. Activation of Rho-kinase inhibits insulin signaling in VSMCs through formation of a complex with IRS-1 (*14*), suggesting that Rho might affect systemic glucose metabolism. Formation of a complex between Rho-kinase and IRS-1 increases serine phosphorylation of IRS-1 and decreases its tyrosine phosphorylation of IRS-1 (*14*). Similar changes in IRS-1 phosphorylation occur in muscle tissue in obese rats and are attenuated by inhibition of Rho-kinase (*11*). Furthermore, long-term treatment with fasudil attenuates weight gain and abdominal fat deposition in Zucker obese rats, although these effects are marginal (*11*) and the direct involvement of Rho–Rho-kinase pathway in adipose tissue has been unclear. Here, we used a mouse model of obesity

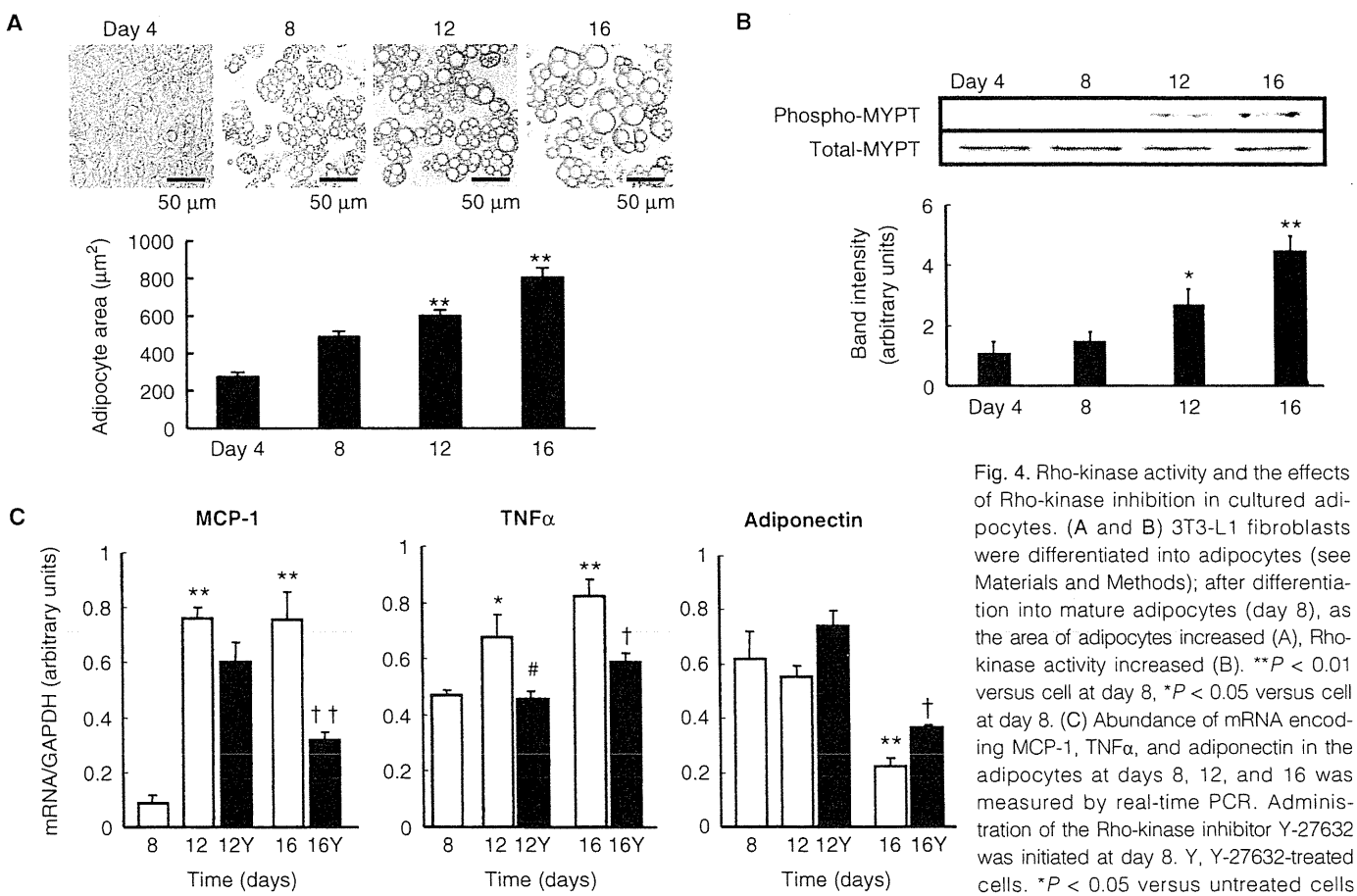

Fig. 4. Rho-kinase activity and the effects of Rho-kinase inhibition in cultured adipocytes. (A and B) 3T3-L1 fibroblasts were differentiated into adipocytes (see Materials and Methods); after differentiation into mature adipocytes (day 8), as the area of adipocytes increased (A), Rho-kinase activity increased (B). $^{**}P < 0.01$ versus cell at day 8, $^{*}P < 0.05$ versus cell at day 8. (C) Abundance of mRNA encoding MCP-1, TNFα, and adiponectin in the adipocytes at days 8, 12, and 16 was measured by real-time PCR. Administration of the Rho-kinase inhibitor Y-27632 was initiated at day 8. Y, Y-27632-treated cells. $^{*}P < 0.05$ versus untreated cells at day 8, $^{**}P < 0.01$ versus untreated cells at day 8, $^{\#}P < 0.05$ versus untreated cells at day 12, $^{\dagger}P < 0.05$ versus untreated cells at day 16, $^{\dagger\dagger}P < 0.01$ versus untreated cells at day 16. $n = 5$.

in response to a HFD to investigate the role of Rho–Rho-kinase signaling in obesity, instead of a genetic model of obesity involving leptin receptor deficiency. We found increased Rho-kinase activity in the adipose tissue of obese mice fed a HFD compared with that in mice fed a LFD. In vitro studies of long-term cultures of adipocytes, as a model of adipocytes in the obese state (*15*), and subfractionation of the adipose tissue of obese mice, revealed that Rho-kinase activation in adipose tissue occurred mainly in adipocytes. Systemic administration of the Rho-kinase inhibitor fasudil blocked activation of Rho-kinase in adipose tissue and attenuated various effects of a HFD in mice, including weight gain, systemic insulin resistance, adipocyte hypertrophy, inflammatory cell infiltration of adipose tissue, and dysregulation of adipocytokine expression. These findings indicate that Rho–Rho-kinase signaling plays a pivotal role in obesity and in the development of obesity-related disorders.

To identify the effects of Rho–Rho-kinase signaling in adipose tissue, we produced transgenic mice that specifically expressed DN-RhoA in adipocytes. Analyses of these mice revealed that specific inhibition of Rho-kinase signaling in adipose tissue inhibited HFD-induced adiposity and weight gain. It also attenuated several metabolic abnormalities associated with obesity induced by a HFD. This implicates activation of this pathway in the adipose tissue as a culprit in the initiation of HFD-induced obesity and obesity-related metabolic disturbances. Several mechanisms likely

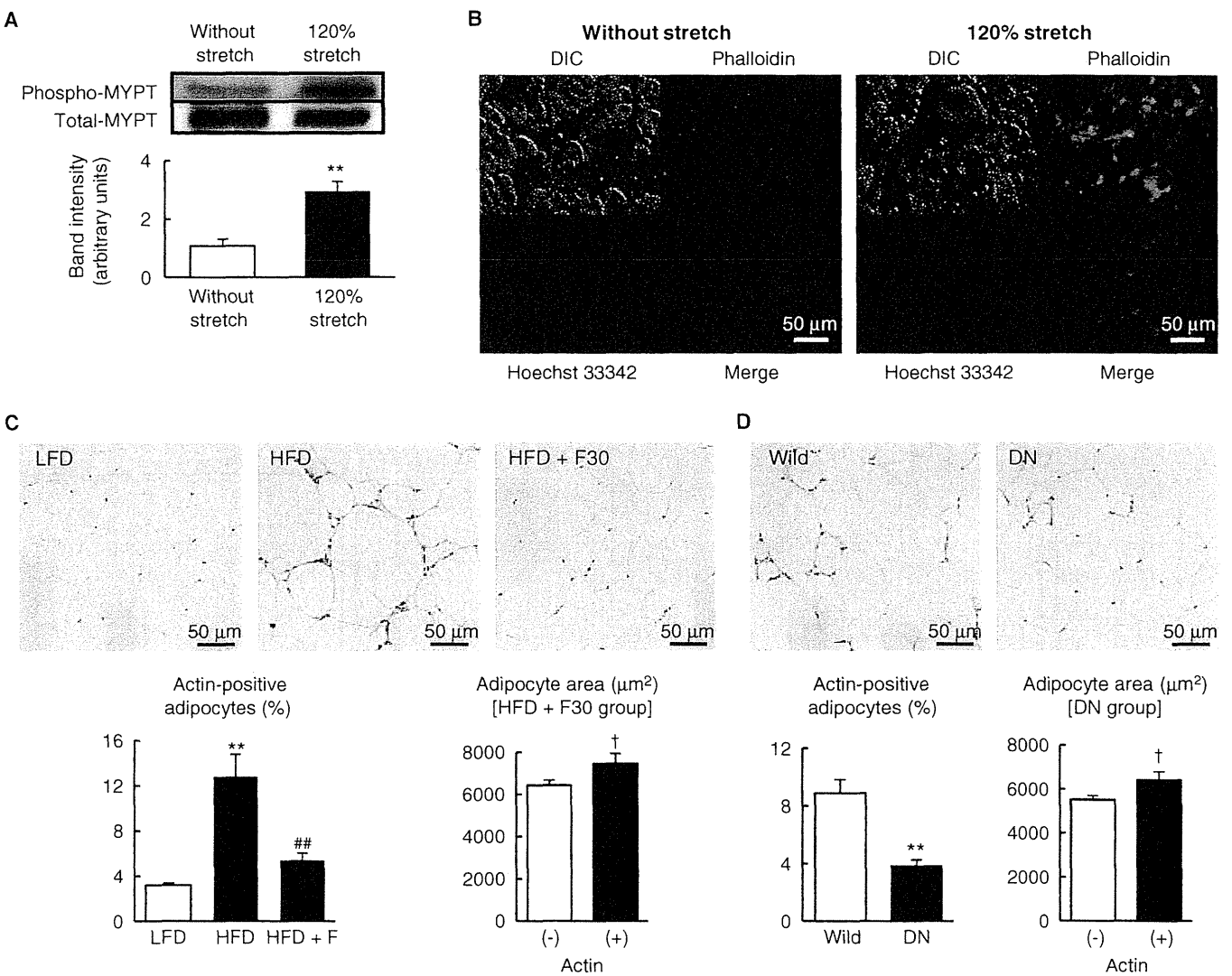

Fig. 5. Mechanical stretch elicited Rho-kinase activity and stress fiber formation in mature adipocytes. (A) Rho-kinase activity was evaluated by immunoblot for phospho-MYPT. $^{**}P < 0.01$ versus without stretch. $n = 4$. (B) Stress fiber formation was detected by rhodamine-labeled phalloidin staining. Nuclear staining was contrasted with stress fiber staining using Hoechst 33342 dye. DIC, differential interference contrast. (C) Actin staining in adipose tissue of mice fed a LFD, obese mice fed a HFD, and fasudil-treated mice fed a HFD. The lower left panel provides quantification, giving the percentage of actin-positive adipocytes. The lower right panel provides the size of actin-positive and -negative adipocytes in the HFD + F30 group. $^{**}P < 0.01$ versus LFD, $^{\#\#}P < 0.01$ versus HFD. $n = 4$. $^{\dagger}P < 0.05$ versus actin-negative adipocytes. $n = 4$. (D) Actin staining in adipose tissue in DN-RhoA TG and wild-type mice. The lower left panel provides quantification. The lower right panel provides the size of actin-positive and -negative adipocytes in the DN group. $^{**}P < 0.01$ versus wild type, $n = 4$. $^{\dagger}P < 0.05$ versus actin-negative adipocytes, $n = 4$.

contributed to the improved glucose metabolism in DN-RhoA TG mice (Fig. 3B). Changes in adipocytokine expression produced by a HFD were partially reversed in DN-RhoA TG mice in a direction that would tend to enhance insulin sensitivity (*16*), as was indeed observed. Increased insulin sensitivity in adipose tissues, as well as the decrease in circulating free fatty acids (Fig. 3C), would also contribute to improved glucose metabolism. DN-RhoA was under the control of the aP2 promoter, which is also expressed in macrophages, lung epithelial cells, and parts of the brain (*17–19*). Therefore, it is conceivable that the changes in adipose tissue phenotype we observed resulted from decreased activation of Rho-kinase in macrophages infiltrating adipose tissues or from alterations in neuronal regulation of adipose tissue. However, Rho-kinase activation in macrophages in HFD-fed obese mice was marginal (Fig. 1G), indicating that the effects of blocking this activation would be limited. Furthermore, any changes in Rho-kinase activity in the central nervous system did not appear to affect appetite or satiety, because food intake between wild-type and DN-RhoA TG mice was similar (wild type, 1.95 ± 0.22 g/day; DN-RhoA TG, 1.86 ± 0.19 g/day). Therefore, we do not consider inhibition of Rho–Rho-kinase pathway in these systems functionally relevant to the obese phenotype in our DN-RhoA TG mice.

DN-RhoA TG mice fed a HFD were leaner than wild-type controls, suggesting the possibility that the reversal of the aberrant HFD-induced adipose tissue phenotype might be secondary to decrease in weight. However, a fasudil dosage of 3 mg/kg per day, which did not affect body weight, attenuated metabolic abnormalities and the aberrant phenotype of adipose tissues in HFD-fed mice (Fig. 1). Similarly, DN-RhoA TG mice were more sensitive to insulin than wild-type mice at a time point when body weight did not differ (Fig. 3, G and H). Thus, we conclude that activation of Rho–Rho-kinase pathway in adipocytes is a culprit in the pernicious phenotype of diet-induced obesity.

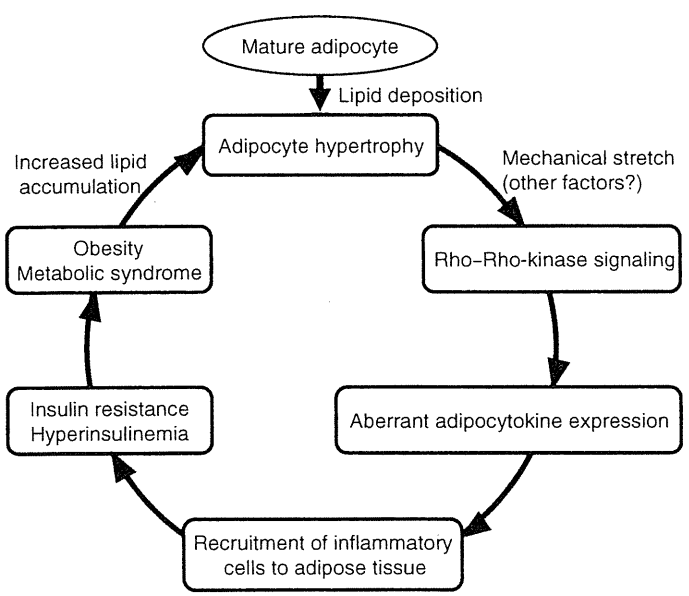

Fig. 6. Schema depicting the vicious cycle of adipose tissues in obesity. After adipocytes mature, increasing lipid accumulation leads to their hypertrophy and consequently to mechanical stretch. Mechanical stretch (and possibly additional factors) promotes Rho-kinase activity, which contributes to aberrant expression of adipocytokines. The acquisition of the hypertrophic phenotype and abnormal adipocytokine secretion, in turn, accelerate inflammation of adipose tissue by inflammatory cells, leading to systemic insulin resistance. Insulin resistance cumulates in obesity and its related pathologies, which further induce adipocyte hypertrophy. This vicious cycle contributes to the initiation and progression of obesity and obesity-related systemic diseases.

What triggers the activation of Rho–Rho-kinase signaling in adipocytes of obese mice? Our data support the hypothesis that mechanical stress caused by hypertrophic change triggers activation of the Rho–Rho-kinase pathway. In obesity, adipocytes are affected by various stresses, including those associated with the state of inflammation caused by the infiltration of inflammatory cells (*20*). Adipocytes undergo an extreme increase in volume in obese subjects (*21*), indicating that they are subjected to hypertrophic stress during the accumulation of fat depots. Here, we showed that mechanical stretch comparable to that elicited by hypertrophy induces the activation of Rho–Rho-kinase signaling. Mechanical stretch might not be the only signal that induces Rho–Rho-kinase activity in hypertrophic adipocytes. For instance, increased insulin concentrations or oxidative stress might also activate Rho signaling. However, we observed similar phenotypic changes in in vitro stretched adipocytes and in vivo hypertrophic adipocytes with similar increases in adipocyte size. These findings, although indirect, indicate that phenotype alteration of hypertrophic adipocytes in vivo may be induced, at least in part, by mechanical stress. Indeed, similar functional alterations in response to mechanical stretch have been shown in other cell types, including VSMCs and endothelial cells (*22*). Demonstration of a direct link between mechanical stress in adipocytes and the progression of obesity-related disorders warrants further investigations.

Activation of Rho–Rho-kinase signaling is critical for cytokine expression in adipocytes. A recent study demonstrated that adipocytokine expression, including that of MCP-1 and plasminogen activator inhibitor type 1 (PAI-1), was increased by Rho–Rho-kinase signaling in cultured adipocytes through activation of nuclear factor κB (NF-κB), a master regulator of cytokine gene expression (*12*, *23*). MCP-1 is also directly regulated by Rho-kinase, as observed in VSMCs (*24*). We propose that, in hypertrophic adipocytes, activation of Rho–Rho-kinase signaling through mechanical stress induces *TNFα* expression—likely through the activation of NF-κB—and also induces *MCP-1* expression, leading to macrophage infiltration into adipose tissue. This enhances inflammatory changes in adipose tissue and aggravates systemic metabolic disturbances including hyperinsulinemia, which inhibits adipocyte lipolysis, leading to additional adipocyte hypertrophy. These events establish a vicious circle culminating in the progression of obesity (Fig. 6). Our data provide evidence for a role of hypertrophic stress in the inflammatory changes that take place in adipose tissue.

The activation of Rho-kinase by Rho inhibits adipogenesis from mesenchymal precursor cells, and Rho activation is suppressed during mesenchymal cell commitment into the adipocyte linage (*25*). During adipocyte differentiation, filamentous actin is converted from long stress fibers to cortical actin. These changes are paralleled by suppression of the ROCK2 isoform of Rho-kinase, and treatment with a Rho-kinase inhibitor inhibits cortical stress fiber formation, implying that Rho–Rho-kinase signaling is also suppressed during adipogenesis (*26*). Our data showed that after adipocyte maturation, long-term culture was associated with increased Rho-kinase activity, indicating that adipocytes acquired the aberrant phenotype associated with adipocyte hypertrophy in obesity (Fig. 5). This phenotypic change is important not only in the pathogenesis of the inflammatory response in adipose tissues, but also for adipocyte survival, because stress fiber formation is crucial for the maintenance of cellular structure (*27*). For instance, the vascular endothelial cells that line blood vessels experience fluid shear as blood flows across their surface. This stimulates RhoA activation and the formation of actin stress fibers, which

are believed to help endothelial cells to remain flat under high fluid shear (*28*, *29*). In cardiomyocytes, RhoA activation is required for cytoskeletal organization and protects against apoptosis (*30*). Because adipocytes are under the stress of cellular hypertrophy (*20*), it can be surmised that Rho–Rho-kinase activation is necessary for the maintenance of cell structure. Rho–Rho-kinase signaling in turn leads to the "hypertrophic adipocyte phenotype" and, consequently, inflammatory changes in adipose tissue. We consistently found that in mature adipocytes, the expression of adiponectin, which is involved in systemic insulin sensitivity, was decreased and that of MCP-1, which initiates tissue inflammatory change, was increased by mechanical stress. These changes in mRNA abundance were considered to reflect the phenotypic changes of adipocytes by mechanical stress. Mechanical stress thus serves as an initial trigger to activate the Rho–Rho-kinase pathway and the subsequent alteration of adipocyte phenotype, including reorganization of the cytoskeleton and aberrant cytokine expression. Indeed, we found that the adipocytes of obese mice fed a HFD showed Rho–Rho-kinase–dependent formation of stress fibers (Fig. 5, C and D).

Rho-kinase is indispensable for glucose transport in myocytes and in adipocytes (*31*), and genetic disruption of the ROCK1 isoform of Rho-kinase leads to insulin resistance (*32*), identifying a physiological role for Rho-kinase in glucose utilization. Here and in a previous study, we showed that, in obesity, activation of Rho-kinase in muscle (*11*) or adipose tissue leads to systemic insulin resistance. Together with data implicating ROCK2 in adipocyte development (*26*), our findings indicate that Rho–Rho-kinase signaling plays multiple—sometimes apparently opposing—roles in glucose metabolism under physiological and pathological conditions.

Obesity increases the risk of comorbid conditions, including cardiovascular disease and diabetes, through mechanisms that remain unclear. The degree of abdominal adiposity, as defined by abdominal circumference or by the area of abdominal adipose tissue, appears to be an important marker for the risk of cardiovascular events (*33*). Our data suggest that activation of the Rho–Rho-kinase pathway in adipocytes promotes the acquisition of the aberrant hypertrophic adipocyte phenotype and is crucial for inflammatory changes in adipose tissue. These inflammatory changes accelerate systemic insulin resistance and additional adipocyte hypertrophy (*4*), contributing to the progression of obesity and its related cardiovascular events (Fig. 6). Rho-kinase inhibitors have been used to treat diseases associated with inflammation including asthma (*34*) and rheumatoid arthritis (*35*). Our data suggest that they may also provide a therapeutic strategy against the initiation and progression of metabolic syndrome.

In conclusion, we implicated Rho–Rho-kinase signaling as a culprit in a vicious circle in obesity composed of adipocyte phenotypic changes, inflammation of adipose tissues, and pathological consequences of obesity. Our data demonstrated that the Rho-kinase inhibitor fasudil blocked this vicious cycle and could thus provide a plausible therapeutic strategy for obesity and related systemic disorders, including insulin resistance and atherosclerosis.

MATERIALS AND METHODS

Plasmids and constructs

In constructing the transgenic expression vector, human dominant-negative RhoA mutant (*36*) (DN-RhoA) (provided by K. Kaibuchi, Nagoya University), was ligated with the mouse aP2 promoter (*37*) (provided by BM. Spiegelman, Harvard University). The ligated DN-RhoA complementary DNA (cDNA) was followed by rabbit β-globin (RBG) poly(A) (polyadenylate) tail, and the clone was designated as aP2–DN-RhoA–RBG poly(A) (Fig. 2A).

Generation of transgenic mice that specifically expressed DN-RhoA in adipose tissue

For the generation of adipose tissue–specific DN-RhoA TG mice, we microinjected the Xho I–Not I fragment of aP2–DN-RhoA–RBG poly(A) into one-cell stage fertilized mouse embryos obtained from superovulated C57BL/6J mice (Fig. 2A). Founder mice were identified by Southern blot analysis of genomic DNA with human RhoA cDNA as a probe (Fig. 2B). The positive DN-RhoA TG founders were crossed with wild-type C57BL/6 mice (Charles River Japan Inc.) to obtain the F1 generation. Genomic DNA was isolated from tail biopsies at 3 weeks of age with a DNeasy kit (Qiagen), and screening of genomic DNA samples was done by polymerase chain reaction (PCR) using transgene-specific oligonucleotide primers, TAATACGACTCACTATAGG (aP2 promoter side) and TTCTGGGG-TCCACTTTTCTG (RhoA gene side) (Fig. 2A), which amplify a 1310–base pair (bp) region spanning the junction between the aP2 promoter and the DN-RhoA gene (Fig. 2A). Genomic DNA was isolated from tail biopsies at 3 weeks of age with a DNeasy kit and subjected to Southern blot analysis to identify the transgene. Southern blots were performed with a ^{32}P-labeled probe composed of 1310 bp of aP2–DN-RhoA gene (Fig. 2B). DN-RhoA expression in different founder lines was confirmed by reverse transcription PCR (RT-PCR) using primer sets specific for the DN-RhoA cDNA (table S1 and Fig. 2C).

Animal experimental protocol

Six-week-old male C57BL/6J mice (CLEA Japan Inc.) were divided into four groups (n = 6 per group) and fed a HFD (60% lard, Research Diets Inc.), a LFD (10% lard, Research Diets Inc.), and a HFD with Rho-kinase inhibitor fasudil (Asahi Kasei) at 3 or 30 mg/kg per day (HFD + F3 and HFD + F30, respectively). Fasudil is the Rho-kinase inhibitor most frequently used in long-term in vivo experiments. Its in vivo metabolite, hydroxyfasudil, is more selective for Rho-kinase than the parent drug; the affinity of hydroxyfasudil for Rho-kinase is 100 times higher than for PKC (protein kinase C) and 1000 times higher than for myosin light-chain kinase (*38*–*40*). After 12 weeks on their respective diets, mice were killed and blood samples and epididymal WAT were obtained (*41*). Body weights and tissue weights of the epididymal WAT were also measured. In experiments with adipose tissue–specific DN-RhoA TG mice, TG mice and their wild-type littermates were maintained on HFDs (60% lard) from 6 to 18 weeks of age. Body weight and chow intake were monitored weekly. At 18 weeks of age, mice were killed and epididymal fat tissues were harvested. This study was performed in accordance with the institutional guidelines of the Animal Care and Experimentation Committee in Keio University.

Glucose and insulin tolerance tests

After 12 weeks on their respective diets, mice fed a LFD, HFD, or HFD plus fasudil were subjected to glucose and insulin tolerance tests (GTT and ITT) as described (*42*). Briefly, glucose (1 g/kg) was injected intraperitoneally and blood samples were collected from a tail vein at various time points. Insulin tolerance test was also performed by injecting regular insulin (0.75 IU/kg body weight; Humulin R, Eli Lilly & Co.) intraperitoneally after a 2-hour fast.

Isolation of mature adipocytes and stromal vascular fraction

Isolation of mature adipocytes and stromal vascular fraction was performed as described (*43*). Adipose tissues were harvested and minced in Krebs-Ringer-bicarbonate-Hepes (KRBH) buffer containing 1% (w/v) bovine serum albumin (BSA) (Sigma). Collagenase (Liberase 3, Roche Diagnostics Corp.) was added to a final concentration of 2 mg/ml, and samples were incubated at 37°C on an orbital shaker for 30 min. Samples

were then passed through a 250-μm nylon mesh filter. The suspension was centrifuged at 300*g* for 1 min. Floating cells were collected as the mature adipocyte fraction, and the pelleted cells were collected as the stromal vascular fraction.

Histological analysis and immunohistochemistry

Portions of epididymal adipose tissue were removed and fixed with 10% formaldehyde and embedded in paraffin. Sections were stained with hematoxylin and eosin. For the detection of macrophage infiltration in adipose tissue, immunohistochemistry was performed with F4/80 antibody, which detected macrophage-specific protein (*44*). The number of F4/80-positive cells was counted in a blinded fashion under a microscope with a 400× objective. More than 50 serial fields were examined in each mouse, and five mice were analyzed per group. Stress fibers were detected by rhodamine-labeled phalloidin staining (*45*) or by immunohistochemistry with an anti-actin antibody (Abcam). Adipocyte size was measured with the software Win Roof (Mitani). Adipocyte area was measured by randomly selecting 50 serial fields with a 400× objective for each mouse; five mice were analyzed in each group. To measure the size of acin-positive and actin-negative adipocytes, we randomly selected more than 50 serial fields with a 400× objective of adipose tissue in the HFD + F30 and DN group.

Cell culture protocol

3T3-L1 fibroblasts (European Collection of Cell Cultures) were cultured in Dulbecco's modified Eagle's medium (DMEM) supplemented with 10% (v/v) newborn calf serum and induced to differentiate into adipocytes by exposure for 2 days to induction medium, DMEM containing 0.25 μM dexamethasone (Nacalai Chemicals), 0.5 mM 3-isobutyl-1-methylxanthine (Nacalai), insulin (10 μg/ml; Lilly), and 10% fetal bovine serum (FBS) (day 0). Two days later, the medium was changed to DMEM containing 10% FBS and insulin (10 μg/ml) (day 2). Two days later, media were changed to DMEM containing 10% FBS only (day 4). Subsequently, media were exchanged every other day until day 14. In this protocol, cells become differentiated into mature adipocytes containing fat droplets at day 8 (*46*). After day 8, increased amounts of fat droplet accumulated and cell size increased. To examine the effects of Rho-kinase inhibition on mature adipocytes, we treated the cells with Rho-kinase inhibitors, Y-27632 (10 μM, Calbiochem) and fasudil (10 μM) after day 8. Cells were harvested at days 4, 8, 12, and 16 and analyzed for Rho-kinase activity and adipocytokine mRNA abundance. We used Y-27632 as a Rho-kinase inhibitor in the in vitro experiments because this reagent is more specific than fasudil itself and is widely used for in vitro experiments.

Mechanical stretch of adipocytes

The application of uniaxial stretch to differentiating 3T3-L1 cells was carried out as described (*47*), except static stretching condition was used in this study. Briefly, 3T3-L1 fibroblasts were cultured in collagen-coated silicon chambers and differentiated into mature adipocytes. On day 12, mature adipocytes were subjected to stretch. Cells were subjected to constant stretching of up to 120% of the initial length for a 72-hour duration, conditions that preserve cell survival and the viability of mature adipocytes (*47*). No apparent sign of cell damage, such as detachment of cells from the substratum, was observed under these conditions. Stretched cells were harvested and subjected to real-time PCR or immunocytochemistry.

Immunoblotting

Immunoblot analysis was performed as described (*48*) with some modifications. Blots were incubated with specific antibodies against Rho-kinase α (BD Biosciences Pharmingen) and MYPT (Santa Cruz Biotechnology). Rho-kinase activity was assessed by phosphorylation of MYPT and ERM with antibodies that specifically recognized MYPT phosphorylation at Thr^{696} (Upstate) (*49*) and ERM phosphorylation at ezrin (Thr^{567}), radixin (Thr^{564}), and moesin (Thr^{558}) (Cell Signaling Technology) (*50*).

RNA extraction and real-time PCR

Total RNA was extracted from mouse adipose tissue with the RNeasy lipid tissue kit (Qiagen). Total RNA was subjected to reverse transcription in a 20-μl reaction containing random primers and Superscript II enzyme (Invitrogen). Quantitative real-time PCR was performed with an ABI Prism 7700 Sequence Detection System using SYBR Green PCR Master Mix Reagent Kit (Applied Biosystems). Primers used are indicated in table S1. PCR-amplified products were also electrophoresed on agarose gels to confirm that single bands were amplified. mRNA expression was normalized to that of *GAPDH* (glyceraldehyde-3-phosphate dehydrogenase).

Statistical analysis

Data are expressed as means ± SEM. Data were analyzed by one- or two-way analysis of variance as appropriate, followed by Bonferroni's post hoc test. $P < 0.05$ was considered statistically significant.

SUPPLEMENTARY MATERIALS

www.sciencesignaling.org/cgi/content/full/4/157/ra3/DC1
Fig. S1. The effects of fasudil on adipocytokine mRNA in mature adipocytes.
Table S1. Primers used in real-time RT-PCR analysis.

REFERENCES AND NOTES

1. A. Lenz, F. B. Diamond Jr., Obesity: The hormonal milieu. *Curr. Opin. Endocrinol. Diabetes Obes.* **15**, 9–20 (2008).
2. N. Rasouli, P. A. Kern, Adipocytokines and the metabolic complications of obesity. *J. Clin. Endocrinol. Metab.* **93**, S64–S73 (2008).
3. F. Lago, C. Dieguez, J. Gómez-Reino, O. Gualillo, Adipokines as emerging mediators of immune response and inflammation. *Nat. Clin. Pract. Rheumatol.* **3**, 716–724 (2007).
4. G. S. Hotamisligil, Inflammation and metabolic disorders. *Nature* **444**, 860–867 (2006).
5. K. E. Wellen, G. S. Hotamisligil, Inflammation, stress, and diabetes. *J. Clin. Invest.* **115**, 1111–1119 (2005).
6. K. Kaibuchi, S. Kuroda, M. Amano, Regulation of the cytoskeleton and cell adhesion by the Rho family GTPases in mammalian cells. *Annu. Rev. Biochem.* **68**, 459–486 (1999).
7. K. Kimura, M. Ito, M. Amano, K. Chihara, Y. Fukata, M. Nakafuku, B. Yamamori, J. Feng, T. Nakano, K. Okawa, A. Iwamatsu, K. Kaibuchi, Regulation of myosin phosphatase by Rho and Rho-associated kinase (Rho-kinase). *Science* **273**, 245–248 (1996).
8. J. Pan, U. S. Singh, T. Takahashi, Y. Oka, A. Palm-Leis, B. S. Herbelin, K. M. Baker, PKC mediates cyclic stretch-induced cardiac hypertrophy through Rho family GTPases and mitogen-activated protein kinases in cardiomyocytes. *J. Cell. Physiol.* **202**, 536–553 (2005).
9. K. Numaguchi, S. Eguchi, T. Yamakawa, E. D. Motley, T. Inagami, Mechanotransduction of rat aortic vascular smooth muscle cells requires RhoA and intact actin filaments. *Circ. Res.* **85**, 5–11 (1999).
10. S. Kawamura, S. Miyamoto, J. H. Brown, Initiation and transduction of stretch-induced RhoA and Rac1 activation through caveolae: Cytoskeletal regulation of ERK translocation. *J. Biol. Chem.* **278**, 31111–31117 (2003).
11. T. Kanda, S. Wakino, K. Homma, K. Yoshioka, S. Tatematsu, K. Hasegawa, I. Takamatsu, N. Sugano, K. Hayashi, T. Saruta, Rho-kinase as a molecular target for insulin resistance and hypertension. *FASEB J.* **20**, 169–171 (2006).
12. Y. Nakayama, R. Komuro, A. Yamamoto, Y. Miyata, M. Tanaka, M. Matsuda, A. Fukuhara, I. Shimomura, RhoA induces expression of inflammatory cytokine in adipocytes. *Biochem. Biophys. Res. Commun.* **379**, 288–292 (2009).
13. Y. He, H. Xu, L. Liang, Z. Zhan, X. Yang, X. Yu, Y. Ye, L. Sun, Antiinflammatory effect of Rho-kinase blockade via inhibition of NF-κB activation in rheumatoid arthritis. *Arthritis Rheum.* **58**, 3366–3376 (2008).
14. N. Begum, O. A. Sandu, M. Ito, S. M. Lohmann, A. Smolenski, Active Rho-kinase (ROK-α) associates with insulin receptor substrate-1 and inhibits insulin signaling in vascular smooth muscle cells. *J. Biol. Chem.* **277**, 6214–6222 (2002).

15. C. Fischbach, T. Spruss, B. Weiser, M. Neubauer, C. Becker, M. Hacker, A. Göpferich, T. Blunk, Generation of mature fat pads in vitro and in vivo utilizing 3-D long-term culture of 3T3-L1 preadipocytes. *Exp. Cell Res.* **300**, 54–64 (2004).
16. M. Fasshauer, R. Paschke, Regulation of adipocytokines and insulin resistance. *Diabetologia* **46**, 1594–1603 (2003).
17. L. Makowski, J. B. Boord, K. Maeda, V. R. Babaev, K. T. Uysal, M. A. Morgan, R. A. Parker, J. Suttles, S. Fazio, G. S. Hotamisligil, M. F. Linton, Lack of macrophage fatty-acid–binding protein aP2 protects mice deficient in apolipoprotein E against atherosclerosis. *Nat. Med.* **7**, 699–705 (2001).
18. B. O. Shum, C. R. Mackay, C. Z. Gorgun, M. J. Frost, R. K. Kumar, G. S. Hotamisligil, M. S. Rolph, The adipocyte fatty acid–binding protein aP2 is required in allergic airway inflammation. *J. Clin. Invest.* **116**, 2183–2192 (2006).
19. A. Mishra, C. H. Cheng, W. C. Lee, L. L. Tsai, Proteomic changes in the hypothalamus and retroperitoneal fat from male F344 rats subjected to repeated light–dark shifts. *Proteomics* **9**, 4017–4028 (2009).
20. A. Rudich, H. Kanety, N. Bashan, Adipose stress-sensing kinases: Linking obesity to malfunction. *Trends Endocrinol. Metab.* **18**, 291–299 (2007).
21. S. L. Gray, A. J. Vidal-Puig, Adipose tissue expandability in the maintenance of metabolic homeostasis. *Nutr. Rev.* **65**, S7–S12 (2007).
22. G. Loirand, P. Guérin, P. Pacaud, Rho kinases in cardiovascular physiology and pathophysiology. *Circ. Res.* **98**, 322–334 (2006).
23. P. L. Rodriguez, S. Sahay, O. O. Olabisi, I. P. Whitehead, ROCK I-mediated activation of NF-κB by RhoB. *Cell. Signal.* **19**, 2361–2369 (2007).
24. Y. Funakoshi, T. Ichiki, H. Shimokawa, K. Egashira, K. Takeda, K. Kaibuchi, M. Takeya, T. Yoshimura, A. Takeshita, Rho-kinase mediates angiotensin II-induced monocyte chemoattractant protein-1 expression in rat vascular smooth muscle cells. *Hypertension* **38**, 100–104 (2001).
25. R. Sordella, W. Jiang, G. C. Chen, M. Curto, J. Settleman, Modulation of Rho GTPase signaling regulates a switch between adipogenesis and myogenesis. *Cell* **113**, 147–158 (2003).
26. M. Noguchi, K. Hosoda, J. Fujikura, M. Fujimoto, H. Iwakura, T. Tomita, T. Ishii, N. Arai, M. Hirata, K. Ebihara, H. Masuzaki, H. Itoh, S. Narumiya, K. Nakao, Genetic and pharmacological inhibition of Rho-associated kinase II enhances adipogenesis. *J. Biol. Chem.* **282**, 29574–29583 (2007).
27. S. Pellegrin, H. Mellor, Actin stress fibres. *J. Cell Sci.* **120**, 3491–3499 (2007).
28. R. P. Franke, M. Gräfe, H. Schnittler, D. Seiffge, C. Mittermayer, D. Drenckhahn, Induction of human vascular endothelial stress fibers by fluid shear stress. *Nature* **307**, 648–649 (1984).
29. B. Wojciak-Stothard, A. J. Ridley, Shear stress–induced endothelial cell polarization is mediated by Rho and Rac but not Cdc42 or PI 3-kinase. *J. Cell Biol.* **161**, 429–439 (2003).
30. D. P. Del Re, S. Miyamoto, J. H. Brown, Focal adhesion kinase as a RhoA-activable signaling scaffold mediating Akt activation and cardiomyocyte protection. *J. Biol. Chem.* **283**, 35622–35629 (2008).
31. N. Furukawa, P. Ongusaha, W. J. Jahng, K. Araki, C. S. Choi, H. J. Kim, Y. H. Lee, K. Kaibuchi, B. B. Kahn, H. Masuzaki, J. K. Kim, S. W. Lee, Y. B. Kim, Role of Rho-kinase in regulation of insulin action and glucose homeostasis. *Cell Metab.* **2**, 119–129 (2005).
32. D. H. Lee, J. Shi, N. H. Jeoung, M. S. Kim, J. M. Zabolotny, S. W. Lee, M. F. White, L. Wei, Y.-B. Kim, Targeted disruption of ROCK1 causes insulin resistance in vivo. *J. Biol. Chem.* **284**, 11776–11780 (2009).
33. J. P. Després, B. J. Arsenault, M. Côté, A. Cartier, I. Lemieux, Abdominal obesity: The cholesterol of the 21st century? *Can. J. Cardiol.* **24** (Suppl. D), 7D–12D (2008).
34. H. Kume, RhoA/Rho-kinase as a therapeutic target in asthma. *Curr. Med. Chem.* **15**, 2876–2885 (2008).
35. Y. He, H. Xu, L. Liang, Z. Zhan, X. Yang, X. Yu, Y. Ye, L. Sun, Antiinflammatory effect of Rho kinase blockade via inhibition of NF-κB activation in rheumatoid arthritis. *Arthritis Rheum.* **58**, 3366–3376 (2008).
36. M. Amano, H. Mukai, Y. Ono, K. Chihara, T. Matsui, Y. Hamajima, K. Okawa, A. Iwamatsu, K. Kaibuchi, Identification of a putative target for Rho as the serine-threonine kinase protein kinase N. *Science* **271**, 648–650 (1996).
37. S. R. Ross, R. A. Graves, A. Greenstein, K. A. Platt, H. L. Shyu, B. Mellovitz, B. M. Spiegelman, A fat-specific enhancer is the primary determinant of gene expression for adipocyte P2 in vivo. *Proc. Natl. Acad. Sci. U.S.A.* **87**, 9590–9594 (1990).
38. Y. Sasaki, M. Suzuki, H. Hidaka, The novel and specific Rho-kinase inhibitor (*S*)-(+)-2-methyl-1-[(4-methyl-5-isoquinoline)sulfonyl]-homopiperazine as a probing molecule for Rho-kinase-involved pathway. *Pharmacol. Ther.* **93**, 225–232 (2002).
39. S. Satoh, T. Utsunomiya, K. Tsurui, T. Kobayashi, I. Ikegaki, Y. Sasaki, T. Asano, Pharmacological profile of hydroxy fasudil as a selective rho kinase inhibitor on ischemic brain damage. *Life Sci.* **69**, 1441–1453 (2001).
40. S. Satoh, T. Yamaguchi, A. Hitomi, N. Sato, K. Shiraiwa, I. Ikegaki, T. Asano, H. Shimokawa, Fasudil attenuates interstitial fibrosis in rat kidneys with unilateral ureteral obstruction. *Eur. J. Pharmacol.* **455**, 169–174 (2002).
41. T. Jiang, Z. Wang, G. Proctor, S. Moskowitz, S. E. Liebman, T. Rogers, M. S. Lucia, J. Li, M. Levi, Diet-induced obesity in C57BL/6J mice causes increased renal lipid accumulation and glomerulosclerosis via a sterol regulatory element-binding protein-1c-dependent pathway. *J. Biol. Chem.* **280**, 32317–32325 (2005).
42. K. Kaku, F. T. Fiedorek Jr., M. Province, M. A. Permutt, Genetic analysis of glucose tolerance in inbred mouse strains. Evidence for polygenic control. *Diabetes* **37**, 707–713 (1988).
43. S. P. Weisberg, D. Hunter, R. Huber, J. Lemieux, S. Slaymaker, K. Vaddi, I. Charo, R. L. Leibel, A. W. Ferrante Jr., CCR2 modulates inflammatory and metabolic effects of high-fat feeding. *J. Clin. Invest.* **116**, 115–124 (2006).
44. W. Khazen, J. P. M'bika, C. Tomkiewicz, C. Benelli, C. Chany, A. Achour, C. Forest, Expression of macrophage-selective markers in human and rodent adipocytes. *FEBS Lett.* **579**, 5631–5634 (2005).
45. A. Masamune, K. Kikuta, M. Satoh, K. Satoh, T. Shimosegawa, Rho kinase inhibitors block activation of pancreatic stellate cells. *Br. J. Pharmacol.* **140**, 1292–1302 (2003).
46. C. X. Andersson, V. R. Sopasakis, E. Wallerstedt, U. Smith, Insulin antagonizes interleukin-6 signaling and is anti-inflammatory in 3T3-L1 adipocytes. *J. Biol. Chem.* **282**, 9430–9435 (2007).
47. Y. Tanabe, Y. Matsunaga, M. Saito, K. Nakayama, Involvement of cyclooxygenase-2 in synergistic effect of cyclic stretching and eicosapentaenoic acid on adipocyte differentiation. *J. Pharmacol. Sci.* **106**, 478–484 (2008).
48. S. Wakino, U. Kintscher, Z. Liu, S. Kim, F. Yin, M. Ohba, T. Kuroki, A. H. Schönthal, W. A. Hsueh, R. E. Law, Peroxisome proliferator-activated receptor γ ligands inhibit mitogenic induction of $p21^{Cip1}$ by modulating the protein kinase Cδ pathway in vascular smooth muscle cells. *J. Biol. Chem.* **276**, 47650–47657 (2001).
49. A. V. Somlyo, C. Phelps, C. Dipierro, M. Eto, P. Read, M. Barrett, J. J. Gibson, M. C. Burnitz, C. Myers, A. P. Somlyo, Rho-kinase and matrix metalloproteinase inhibitors cooperate to inhibit angiogenesis and growth of human prostate cancer xenotransplants. *FASEB J.* **17**, 223–234 (2003).
50. T. Matsui, M. Maeda, Y. Doi, S. Yonemura, M. Amano, K. Kaibuchi, S. Tsukita, S. Tsukita, Rho-kinase phosphorylates COOH-terminal threonines of ezrin/radixin/moesin (ERM) proteins and regulates their head-to-tail association. *J. Cell Biol.* **140**, 647–657 (1998).

51. **Acknowledgments:** We thank Y. Ogawa and T. Suganami from Tokyo Medical and Dental University for helpful discussions. We are also grateful to M. Amano from Nagoya University for providing information on the dominant-negative human RhoA construct. **Funding:** This work was supported by research funding from the Ministry of Education, Culture, Sports, Science and Technology, Japan. **Author contributions:** Y.H., S.W., H.T., S.T., and K.Y. did most of the experiments. Y.T. and M.S. did the cell stretch experiments. N.W., K. Homma, K. Hasegawa, H.M., K.F., and K. Hosoya did animal bleeding and assisted in the experiments. K.N. provided the stretch device. Y.H., S.W., K. Hayashi, and H.I. conceived and designed the project and wrote the manuscript. **Competing interests:** The authors declare that they have no competing interests.

Submitted 2 June 2010
Accepted 5 January 2011
Final Publication 25 January 2011
10.1126/scisignal.2001227
Citation: Y. Hara, S. Wakino, Y. Tanabe, M. Saito, H. Tokuyama, N. Washida, S. Tatematsu, K. Yoshioka, K. Homma, K. Hasegawa, H. Minakuchi, K. Fujimura, K. Hosoya, K. Hayashi, K. Nakayama, H. Itoh, Rho and Rho-kinase activity in adipocytes contributes to a vicious cycle in obesity that may involve mechanical stretch. *Sci. Signal.* **4**, ra3 (2011).

NDT Advance Access published March 4, 2011

Nephrol Dial Transplant (2011) 0: 1–10
doi: 10.1093/ndt/gfr012

NDT
Nephrology Dialysis Transplantation

Original Article

Rho-kinase inhibition ameliorates peritoneal fibrosis and angiogenesis in a rat model of peritoneal sclerosis

Naoki Washida[1], Shu Wakino[1], Yukio Tonozuka[2], Koichiro Homma[1], Hirobumi Tokuyama[1], Yoshikazu Hara[1], Kazuhiro Hasegawa[1], Hitoshi Minakuchi[1], Keiko Fujimura[1], Kohji Hosoya[1], Koichi Hayashi[1] and Hiroshi Itoh[1]

[1]Department of Internal Medicine, School of Medicine, Keio University, Tokyo, Japan and [2]Baxter Inc., Tokyo, Japan

Correspondence and offprint requests to: Shu Wakino; E-mail: swakino@sc.itc.keio.ac.jp

Abstract

Background. Peritoneal fibrosis (PF) and angiogenesis are typical morphological changes, leading to loss of peritoneal functions in patients undergoing peritoneal dialysis. The small G protein, Rho, and its downstream effector Rho-kinase have been shown to be involved in the tissue fibrosis process. This study was undertaken to investigate the role of Rho-kinase in the pathogenesis of these alterations.

Methods. PF was induced by intraperitoneal administration of chlorhexidine (CHX) in male rats (CHX group). These rats were treated with a Rho-kinase inhibitor, fasudil (Fas group). Human pleural mesothelial cells, MeT-5A cells, were stimulated by glucose with or without another Rho-kinase inhibitor, Y-27632.

Results. Peritoneal damage including peritoneal thickening, fibrous changes, macrophage migration and angiogenesis were evident in the CHX group and were ameliorated in the Fas group. The expression of markers of tissue fibrosis, such as transforming growth factor (TGF)-β, fibronectin and α-smooth muscle cell actin, were increased in the CHX group and were downregulated by fasudil. Similar results were also seen with an inducer of angiogenesis, vascular endothelial growth factor (VEGF). Rho-kinase was activated in the peritoneum of the CHX group, which was inhibited by fasudil. In MeT-5A cells, high glucose increased TGF-β expression and VEGF secretion, which were blocked by Y-27632.

Conclusions. The activation of Rho-kinase is involved in peritoneal damage at multiple stages including tissue fibrosis and angiogenesis. The inhibition of Rho-kinase constitutes a novel strategy for the treatment of PF.

Keywords: angiogenesis; peritoneal dialysis; peritoneal fibrosis; peritonium; Rho-kinase inhibitor

Introduction

Peritoneal dialysis (PD) is one treatment of choice of the treatments for end-stage renal failure. One of the long-term complications of PD is the decline of peritoneal function [1]. The decrease in ultrafiltration capacity after prolonged PD is an important reason for its discontinuation. Long-term PD is accompanied by functional and histopathological alterations in the peritoneum. Chronic peritoneal damage in PD is associated with multiple factors, including peritoneal fibrosis (PF), epithelial-messenchymal transition (EMT) of mesothelial cells and peritoneal neovascularization [2]. The pathogenesis of PF is a combination of bioincompatible factors in the dialysate, including high glucose, high osmolality, advanced glycation products, glucose degradation products, uremic inflammation and acute peritonitis with inflammation [3]. A previous study demonstrated that glucose or glucose degradation products stimulate the production of transforming growth factor (TGF)-β, fibronectin and vascular endothelial growth factor (VEGF) from peritoneal mesothelial cells, which aggravated the progression of PF [4–7]. TGF-β has been reported to play a central role in tissue fibrosis, leading to a progressive loss of mesothelial cells [8]. Local production of VEGF plays a pivotal role in the angiogenesis of peritoneal tissues [9]. The expansion of the peritoneal vasculature is the main determinant of increased solute transport across the peritoneum that inhibits ultrafiltration capacity [10].

A serious complication of long-term PD is the development of encapsulating peritoneal sclerosis (EPS), which is characterized by bowel obstructions, various degrees of inflammation and enormous peritoneal thickening and encapsulation and cocooning [11]. It is also sometimes accompanied by peritoneal calcification [11]. These advanced lesions of PD complication need to be differentiated from PF and the final histological change of PF, peritoneal sclerosis (PS), as often seen in long-term PD patients without EPS [1]. Several factors were considered to be involved in the development of EPS, including PF, although the precise mechanisms have not yet been determined [12].

Small GTPase Rho-kinase, a member of the Rho-kinase subfamily of the Ras superfamily of monomeric GTPases, constitutes an important modulator of vascular smooth

muscle contraction [13]. Rho-kinase and its downstream effector Rho-kinase are important mediators not only of vascular contraction but also of actin cytoskeleton reorganization, cellular morphology, motility, adhesion and proliferation [14]. Because of its effects on various cellular functions, Rho-kinase has attracted significant interest as a potential target for the treatment of a wide range of pathological conditions including cancer, neuronal degeneration, kidney failure, asthma, glaucoma, osteoporosis, erectile dysfunction, insulin resistance and surgical adhesion. In practice, Rho-kinase inhibitor, fasudil, has already been in use for the prevention of vasospasm after the attack of subarachnoid hemorrhage [15]. One of the areas of interest has been their potential use for the prevention against the tissue fibrosis [16, 17].

Recent studies have witnessed that the Rho/Rho-kinase pathway is associated with tissue fibrosis and inflammation. It has also been demonstrated that the Rho/Rho-kinase pathway is involved in the tissue fibrosis process in various tissues through the regulation of TGF-β activation [18–20]. Y-27632, a specific Rho-kinase inhibitor, prevented the upregulation of α-smooth muscle actin (α-SMA), a marker of tissue fibrosis and inhibited tubulointerstitial fibrosis in mouse kidneys with unilateral ureteral obstruction [16]. In addition, the Rho/Rho-kinase pathway regulates hypoxia-induced VEGF expression [21]. These data in concert, suggested that Rho/Rho-kinase is involved in a final common pathway that aggravates the progression of peritoneal dysfunction.

Previously, we demonstrated that the Rho/Rho-kinase pathway is activated in the kidneys of subtotal nephrectomized rats, and the Rho-kinase inhibitor, fasudil, attenuated renal damage in the nephrectomized rats through amelioration of inflammatory changes of remnant kidneys [22]. In the present study, we investigated whether blocking of Rho-kinase similarly inhibited peritoneal damage by using both *in vivo* and *in vitro* systems. While a specific inhibitor, Y-27632 was administered in *in vitro* experiments to block Rho-kinase, we used fasudil in *in vivo* systems, although it is less specific for Rho-kinase. Fasudil is the Rho-kinase inhibitor practically available for long-term *in vivo* use. In addition, when it is administered *in vivo*, its metabolite, hydroxyfasudil, possesses a more selective action than its parent drug on Rho-kinase (specificity for Rho-kinase is 100 times higher for protein kinase C and 1000 times higher for myosin light chain kinase [23]). For these reasons, we selected fasudil to examine the effects of blocking Rho/Rho-kinase pathway *in vivo*. Our data demonstrated that Rho-kinase inhibitors ameliorated peritoneal damages and PF through direct effects on mesothelial cells.

Methods

Animals and peritoneal fibrosis model

Male Wistar rats (Saitama SLC, Saitama, Japan), weighing 150–200 g, were housed in a controlled environment, fed a standard rat chow (0.19% sodium, 0.74% potassium and 20.6% protein; Oriental Yeast Co., Itabashi, Tokyo) and allowed free access to water. Peritoneal inflammation and a sclerosis model was made by injection of a chlorhexidine (CHX) solution consisting of 0.1% CHX gluconate and 15% ethanol intraperitoneally for 4 weeks to male Wister rats at the age of 6 weeks [22, 23]. The rats were fed a standard laboratory diet and allowed free access to water. The rats were treated daily with CHX solution into the peritoneal cavity. The animals were sacrificed 4 weeks after the first CHX solution injection and the peritoneal tissues were dissected carefully for further analysis. All experiments were performed in accordance with the animal experimentation guideline of Keio University School of Medicine.

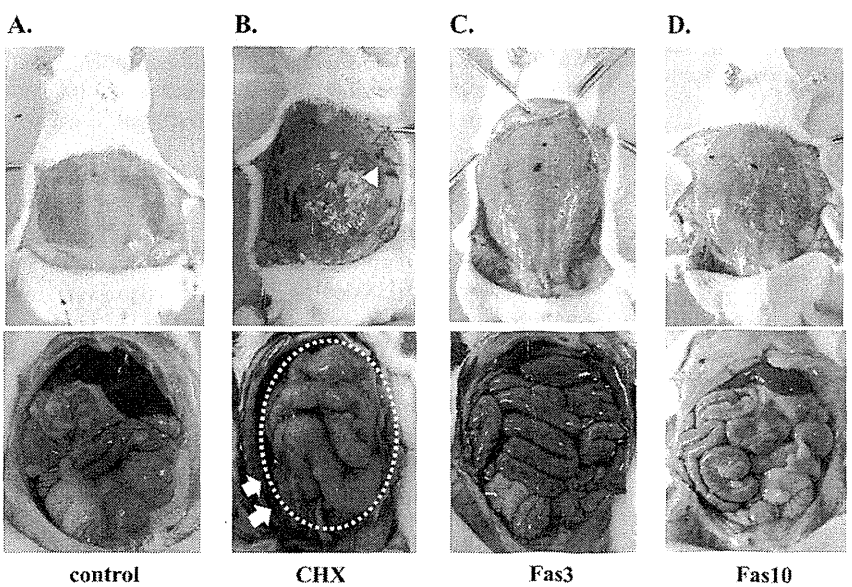

Fig. 1. The effects of the Rho-kinase inhibitor, fasudil, on the macroscopic findings of CHX-induced peritoneal damage. PF was induced in male Wister rats with an intraperitoneal injection of CHX for 4 weeks (**B**). Control rats were subjected to saline injection (**A**). Severe inflammatory changes of peritonium was evident and presented with bowel dilatation, calcification (white triangles), ascites with bleeding (white arrows) and cocoon formation (dotted lined circle). Treatment with fasudil at dosages of 3 mg/kg (Fas3; **C**) and 10 mg/kg (Fas10; **D**) ameliorated these peritoneal damages. Each photograph showed the representative peritoneum (upper panel) and bowel (lower panel) finding in each group.

Animal study protocol

Rats were assigned to four groups: Group 1, rats injected with 2 mL of normal saline (control group, $n = 6$); Group 2, rats injected intraperitoneally with CHX solution (CHX group, $n = 6$); Group 3, rats injected intraperitoneally with CHX solution and 3 mg/kg/day Rho-kinase inhibitor, fasudil (Asahi Kasei, Tokyo, Japan) (Fas3 group, $n = 6$) and Group 4, rats injected intraperitoneally with CHX solution and 10 mg/kg/day fasudil (Fas10 group, $n = 6$). The dosage of fasudil was determined in agreement with previous reports [20, 21].

Histological examination and immunohistochemistry

At sacrifice, intraperitoneal macroscopic views were compared among the four groups. We defined the rats with EPS-like changes as those showing three of five findings: peritoneal calcification, bowel dilatation, bowel adhesion, ascites with bleeding and cocoon formation. We counted the affected rats in each group ($n = 6$), although the extent of peritoneal changes in each rat were different in each group. Three pieces of the mid-parietal peritoneal membrane adjacent to the rectus abdominal muscle were excised. One of these pieces was fixed in 10% buffered formaldehyde, embedded in paraffin and stained with Masson's trichrome solution. Submesothelial thickening was identified as the membrane area extending from the surface mesothelium to the upper limit of the muscular tissues. We measured peritoneal thickness at six random points. Quantification of fibrous tissue area was performed by measuring the Masson's trichrome-stained area at 20 consecutive fields of peritoneal tissues of each group. The number of vessels in the submesothelial zone outside the muscle layer was counted in 10 fields of peritoneal tissues of each group. Fibrous tissue area, peritoneal thickness and the number of vessels were evaluated by Win Roof ver. 6.0 software (Mitani Corp., Tokyo, Japan). These analyses were performed on an individual rat by two investigators in a blinded fashion. Other pieces were embedded in paraffin and used for immunostaining using antibodies against CD68 (AbDserotec, Oxford, UK) and α-SMA (Dako Cytomation, Glostrup, Denmark). Cells stained with α-SMA were counted by computer-aided planimetry using the Scion Image software.

Cell culture and experimental protocols

The human pleural mesothelial cell line MeT-5A was purchased from American Type Culture Collection (Rockville, MD) and cultured in Dulbecco's modified Eagle's medium Nutrient Mixture F-12 (GIBCO) with 10% fetal calf serum, penicillin and streptomycin in a humidified 5% CO2 incubator at 37°C [23, 25]. Although this cell line is derived from pleural tissues, it was utilized because its response to the cellular external stress was demonstrated to be similar to primary peritoneal mesothelial cells [26, 27] and because it showed high viability and good biological response to glucose stimulation. The cells were seeded at a density of 1×10^5 cells per well on a 48-well plate. After MeT-5A cells were grown to 60–70% confluence and made quiescent by serum starvation (0.4%, fetal bovine serum) and normal glucose conditions (5 mmol/L) for 24 h, Rho-kinase inhibitor, Y-27632, was added at three different concentrations of 1, 5 and 10 μmol/L. Thirty minutes after treatment with Y-27632, cells were stimulated with a high concentration of glucose (200 mmol/L) [28]. Eight hours after stimulation, cell lysates were obtained for further analysis [29]. Cell

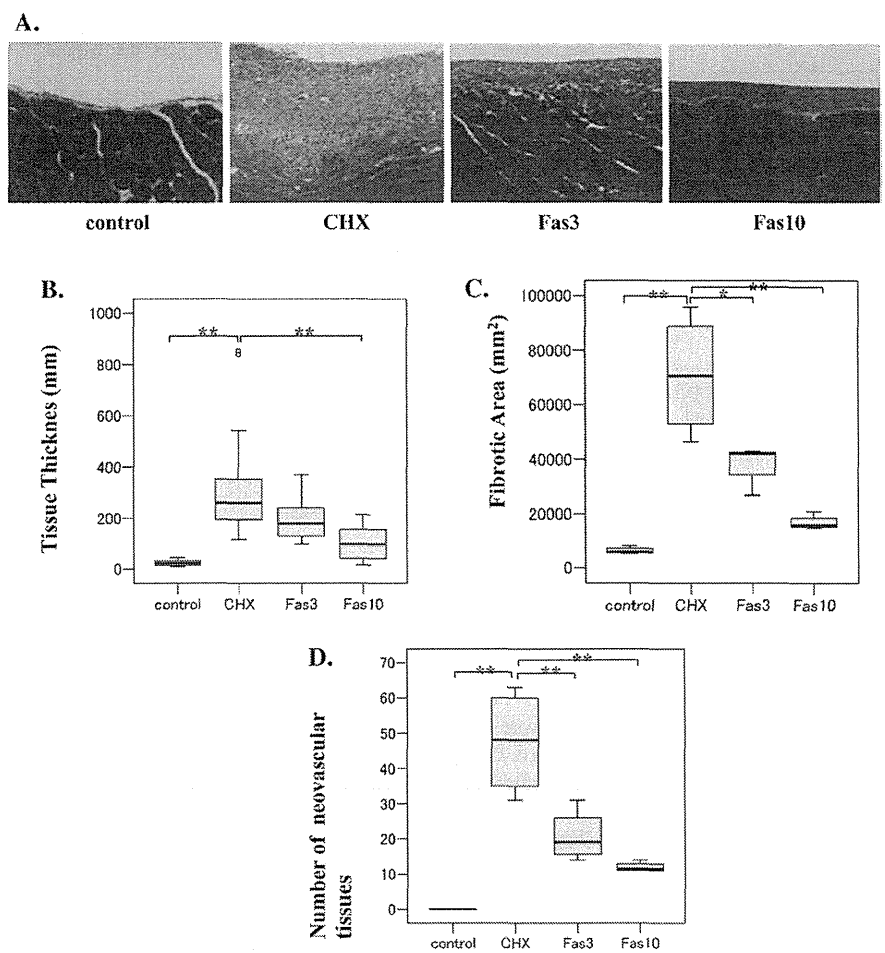

Fig. 2. The effects of fasudil on the histological changes of CHX-induced peritoneal damage. (**A**) Histological findings of the anterior abdominal wall stained with Masson's trichrome solution. Thickness of the peritoneum (**B**), area of fibrous tissues (**C**) and the number of neovascular tissues (**D**) were analyzed in control rats (control), rats with CHX-induced peritoneal damage (CHX) and rats with peritoneal damage treated with 3 mg/kg (Fas3) and 10 mg/kg (Fas10) of fasudil. **P < 0.01 versus CHX group, *P < 0.05 versus CHX group, $n = 6$.

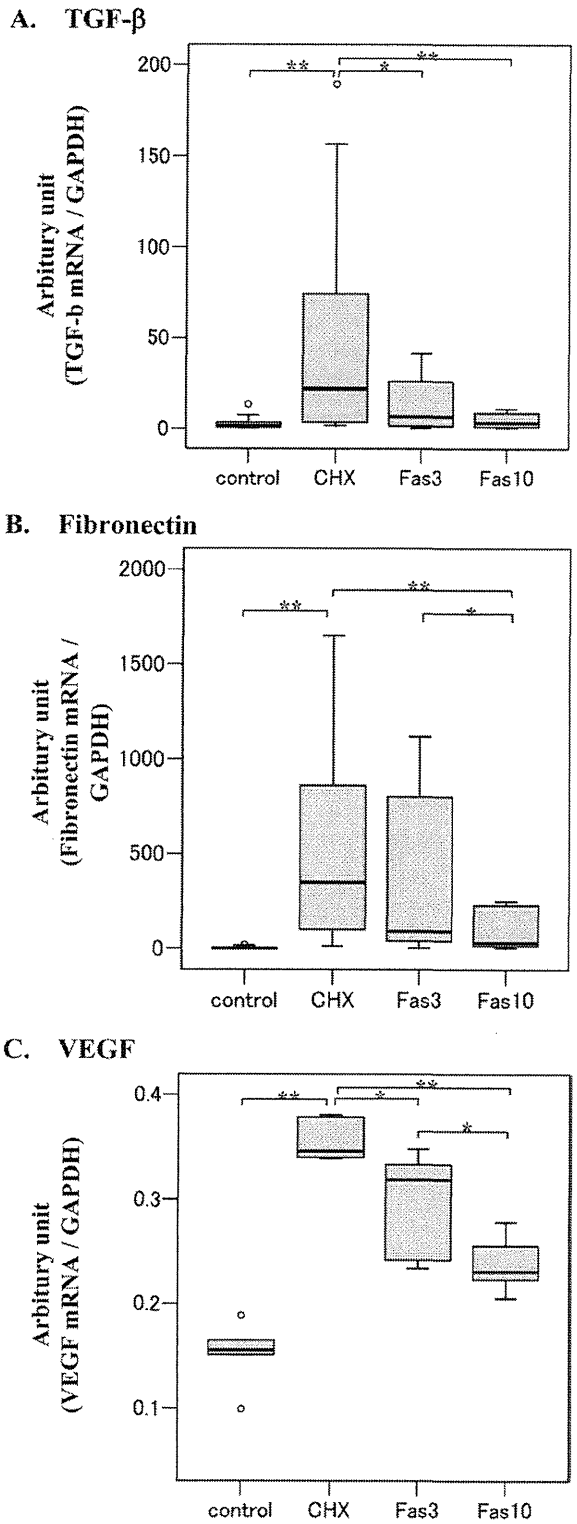

Fig. 3. The effects of fasudil on the mRNA expressions of TGF-β, fibronectin and VEGF in peritoneal tissues. The mRNA expression of TGF-β (**A**), fibronectin (**B**) and VEGF (**C**) in the peritoneal tissues were measured by real-time PCR as described in the Methods section in control rats (control), rats with CHX-induced peritoneal damage (CHX) and rats with peritoneal damage treated with 3 mg/kg (Fas3) and 10 mg/kg (Fas10) of fasudil. **P < 0.01 versus CHX group, *P < 0.05 versus CHX group, $n = 6$.

culture supernatants were also obtained 24 h after stimulation to measure the concentration of VEGF with the quantitative sandwich enzyme immunoassay technique (Quantikine; R&D Systems).

RNA extraction and real-time polymerase chain reaction

Total RNA was extracted from the rat mid-parietal peritoneal tissues with the adjacent muscle tissues using TRIzol reagent [28]. Equal amounts (2 μg) of total RNA from each sample were converted to complementary DNA by M-MLV reverse transcriptase RNaseH with oligo dT20 primer (Invitrogen, Carlsbad, CA) in a 20 μL reaction volume. Real-time polymerase chain reaction (PCR) was performed using LightCycler quick systems 350S (Roche Diagnostics, Tokyo, Japan). Amplification products were analyzed by a melting curve, which confirmed the presence of a single PCR product in all reactions. Levels of messenger RNA (mRNA) were normalized to those of glyceraldehyde 3-phosphate dehydrogenase (GAPDH). The primer sequences were as follows: TGF-β1, sense 5′-AGAAGTCACCCG-CGTGCTAA-3′ and antisense 5′-TCCCGAATGTCTGACGTATTGA-3′; fibronectin, sense 5′-GTGTCTCCAGCGTGTACGAA-3′ and antisense 5′-GGCGGTGACATCAGAAGAAT-3′; VEGF, sense 5′-CATGC-CAAGTGGTCCCA-3′ and antisense 5′-CTATCTTTCTTTGGTCTG-CATTCAC-3′; α-SMA, sense 5′-TGCTGGACTCTGGAGATG-3′ and antisense 5′-GTGATCACCTGCCCATC-3′; GAPDH, sense 5′-CCTGCCAAGTATGATGACATCAAGA-3′ and antisense 5′-GTAGCC-CAGGATGCCCTTTAGT-3′. The amplification program was 95°C for 3 min and then 40 cycles consisting of 95°C for 10 s, 62°C for 10 s and 72°C for 10 s.

Immunoblotting analysis to evaluate the activity of Rho-kinase was performed as described previously [28] by using rat mid-parietal peritoneal tissues with the adjacent muscle tissues. Peritoneal tissues were lysed in 500 μL of ice-cold lysis buffer and centrifuged at 15 000 *g* for 20 min. Supernatant aliquots were subject to immunoblotting using primary antibody against phosphorylated myosin phosphatase target subunit (MYPT1), Rho-kinase substrate (Millipore, Billerica, MA). After the incubation with primary antibody blots were incubated with secondary antibody (horseradish peroxidase-conjugated donkey anti-rabbit IgG; Millipore). Immunoreactive bands were detected using an ECL detection kit (Millipore). Band intensity was determined by using NIH image software (version 1.6).

Data analysis

Statistical analysis was performed using the SPSS 12 software package (SPSS, Chicago, IL). Results are expressed as mean ± SEM of at least three individual experiments. Statistical analysis was performed with analysis of variance followed by Tukey's post-hoc test unless otherwise stated. Differences with $P < 0.05$ were considered statistically significant.

Results

Effects of fasudil on the macroscopic view of peritoneal fibrosis

Four-week intraperitoneal administration with CHX solution induced PS with bowel dilatation, bowel adhesion, peritoneal calcification (Figure 1B, white triangle), ascites with bleeding (Figure 1B, white arrows) and cocoon formation (Figure 1B, dotted lined circle). These findings were similar to those in the patients with EPS (Figure 1). Five of six rats (83.3%) in the CHX group had peritoneal damage which was defined as the rats showing three of five peritoneal and bowel findings as described above. These changes were attenuated by treatment with fasudil in a dose-dependent manner. Thus, two of six rats were affected by the treatment with 3 mg/kg fasudil (Fas3; 33.3%) and none of the six rats by the treatment with 10 mg/kg fasudil (Fas10).

Effects of fasudil on the peritoneal histological changes

After 4-week administration of CHX, peritoneal samples showed markedly increased peritoneal thickness with

mean thickness of 307.6 ± 123.7 μm as compared to that of control rats (22.9 ± 6.7 μm) (Figure 2B, $P < 0.001$, $n = 6$). Treatment with fasudil ameliorated these changes in a dose-dependent manner (Figure 2B, Fas3 group: 185.2 ± 67.1 μm; Fas10 group: 111.5 ± 48.1 μm; $P < 0.001$ versus CHX group, $n = 6$). Masson's trichrome staining revealed that the fibrous area in the submesothelial compact zone of the rats' peritoneum in the CHX group was significantly increased as compared to that of control rats (Figure 2C, control versus CHX: 5815.2 ± 1551.9 μm^2 versus 62 462.3 ± 21 941.2 μm^2, $P < 0.001$, $n = 6$). These increases of tissue fibrotic changes were ameliorated by the treatment with fasudil in a dose-dependent manner (Figure 2C, Fas3 group: 35 666.2 ± 9188.5 μm^2, $P < 0.01$ versus CHX group, $n = 6$; Fas10 group: 16 859.0 ± 2698.7 μm^2, $P < 0.001$ versus CHX group, $n = 6$). Neovascularization of the peritoneum is also characteristic of CHX-induced peritoneal fibrosis as well as peritoneal damage observed in long-term PD patients. The number of vessels, determined by immunostaining with CD31, in the peritoneum of CHX-group rats was increased compared to that of control rats (Figure 2D, control versus CHX: 0.2 ± 0.4/high power field (HPF) versus 43.5 ± 13.3/HPF, $P < 0.001$, $n = 6$ for each group), which was also attenuated by treatment with fasudil in a dose-dependent manner (Figure 2D, Fas3 group: 20.0 ± 6.6/HPF, $P < 0.001$ versus CHX group, $n = 6$ for each group, Fas10 group: 12.0 ± 1.4/HPF, $P < 0.001$ versus CHX group, $n = 6$ for each group).

Effects of fasudil on the expressions of TGF-β, fibronectin and VEGF in peritoneal tissues

The molecular mechanism(s) for the histological improvement by fasudil was investigated by examining the expression of TGF-β and VEGF, humoral mediators for fibrosis and neovascularization, respectively. The mRNA level of TGF-

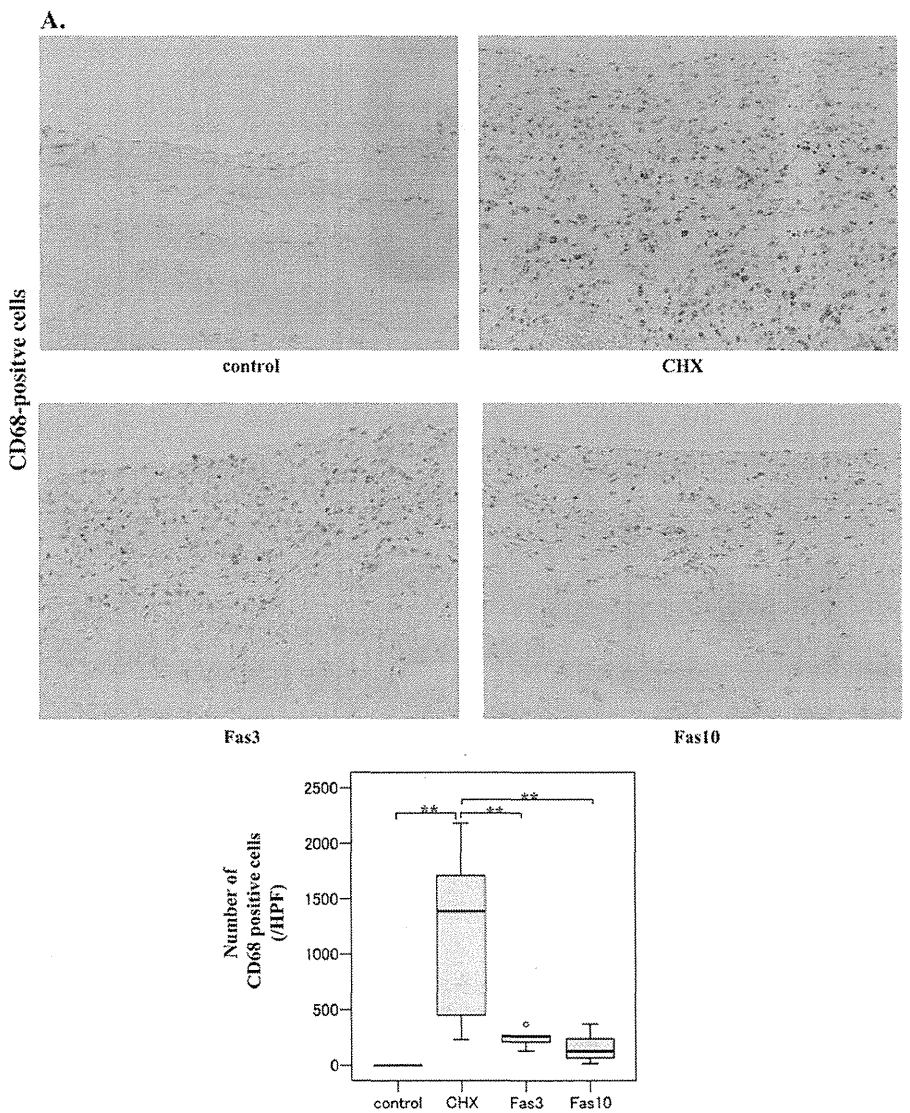

Fig. 4. Continued on following page

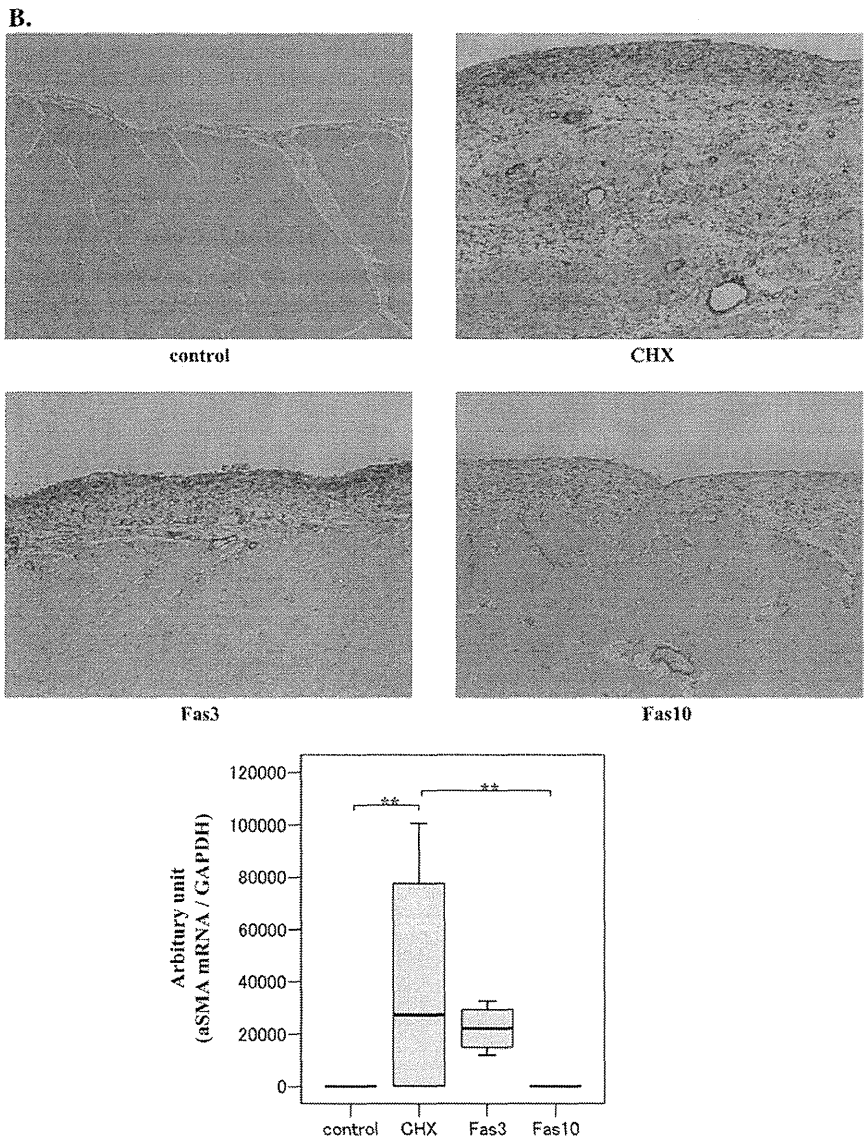

Fig. 4. The effects of fasudil on inflammatory and fibrotic changes in CHX-damaged peritoneal tissues. (**A**) Immunohistochemical analysis by CD68 staining is shown in the upper panel. The number of CD68-positive macrophages were quantified and compared among the control rats (control), rats with CHX-induced peritoneal damage (CHX) and rats with peritoneal damage treated with 3 mg/kg (Fas3) and 10 mg/kg (Fas10) of fasudil (lower panel). **P < 0.01 versus CHX group, *P < 0.05 versus CHX group, $n = 6$. (**B**) Immunohistochemical analysis by α-SMA staining is shown in the upper panel. The mRNA expression of α-SMA was quantified by real-time PCR among control rats (control), rats with CHX-induced peritoneal damage (CHX) and rats with peritoneal damage treated with 3 mg/kg (Fas3) and 10 mg/kg (Fas10) of fasudil (lower panel). **P < 0.01 versus CHX group, *P < 0.05 versus CHX group, $n = 6$.

β was increased in the peritoneum of rats in the CHX group 10.3-fold, which was attenuated by treatment with fasudil in a dose-dependent manner (Figure 3A, Fas3 group: 62.2% inhibition, P < 0.05 versus CHX group, $n = 6$; Fas10 group: 84.2% inhibition, P < 0.01 versus CHX group, $n = 6$). Consistently, mRNA expression of fibronectin, a marker of tissue fibrotic changes, of rats in the CHX group was upregulated 75.4-fold as compared with that in the control group (P < 0.01, $n = 6$). Treatment with fasudil attenuated the increased expression of fibronectin in a dose-dependent manner (Figure 3B, Fas3 group: 20.9% inhibition, P < 0.05 versus CHX group, $n = 6$; Fas10 group: 80.0% inhibition, P < 0.01 versus CHX group, $n = 6$). Similarly, mRNA expression of VEGF was increased in the peritoneum of rats in the CHX group 2.1-fold, which was attenuated by treatment with fasudil in a dose-dependent manner (Figure 3C, Fas3 group: 18.1% inhibition, P < 0.05 versus CHX group, $n = 6$; Fas10 group: 34.9% inhibition, P < 0.01 versus CHX group, $n = 6$).

Effects of fasudil on inflammatory changes and EMT in the CHX-damaged peritoneal tissues

Fibrotic changes of the peritoneum are preceded partly by inflammation of the peritoneum. To assess inflammatory